European Commission

JRC TECHNICAL REPORTS

Quality Assurance for Essential Climate Variables (QA4ECV)

Validation Report for BS FAPAR AVHRR

Gobron, N., Adams J., Lanconelli C., Marioni, M., Robustelli, M. and Vermote E.

2018

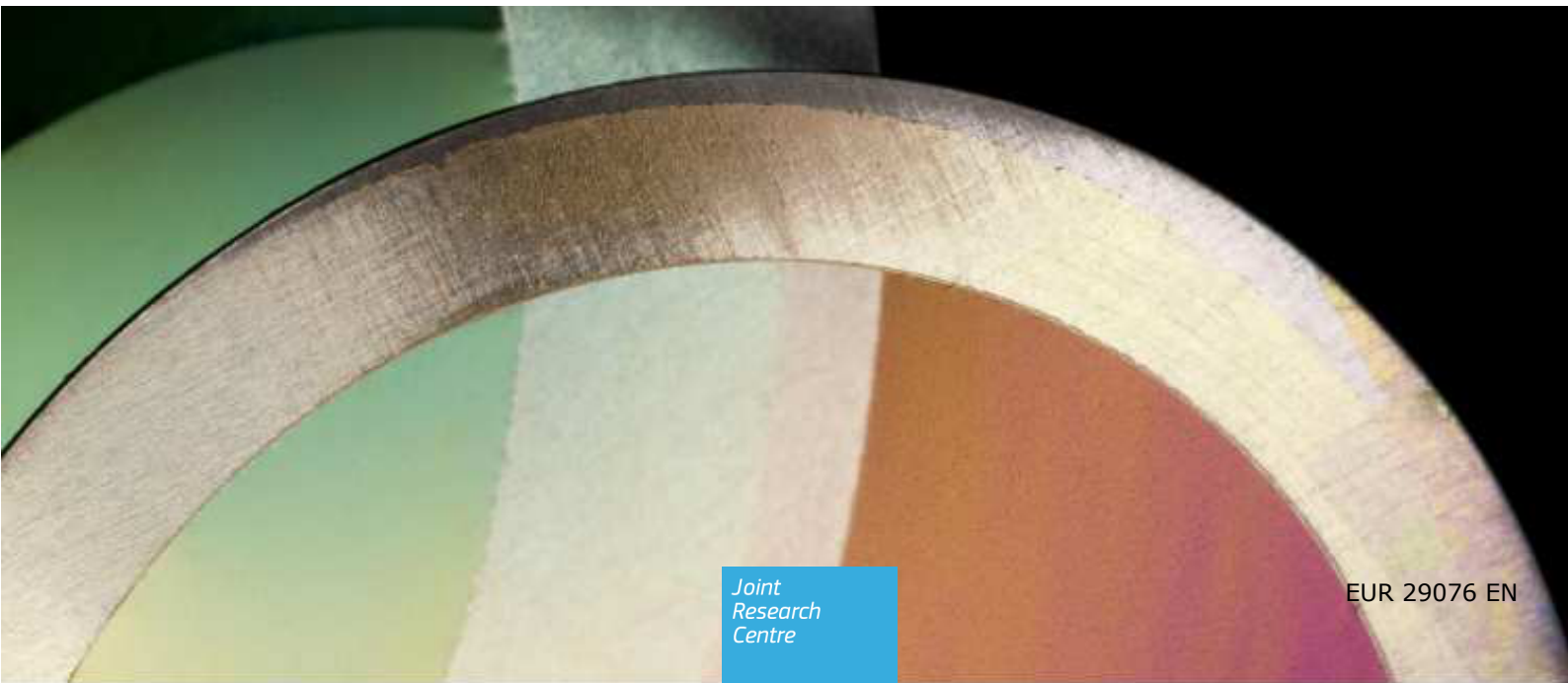

Joint Research Centre

EUR 29076 EN

This publication is a Technical report by the Joint Research Centre (JRC), the European Commission's science and knowledge service. It aims to provide evidence-based scientific support to the European policymaking process. The scientific output expressed does not imply a policy position of the European Commission. Neither the European Commission nor any person acting on behalf of the Commission is responsible for the use that might be made of this publication.

Contact Information
Name: Nadine Gobron
Address: Joint Research Centre, Via Enrico Fermi 2749, TP 123, 21027 Ispra (VA), Italy
E-mail: nadine.gobron@ec.europa.eu
Tel.: +39 0332 786338

EU Science Hub
https://ec.europa.eu/jrc

JRC110486

EUR 29076 EN

PDF ISBN 978-92-79-77731-8 ISSN 1831-9424 doi:10.2760/28321

Luxembourg: Publications Office of the European Union, 2018

How to cite this report: Gobron N., Adams J., Lanconelli C., Marioni, M., Robustelli, M. and Vermote E., Validation Report for QA4ECV BS FAPAR AVHRR, EUR 29076 EN, Publications Office of the European Union, Luxembourg, 2018, ISBN 978-92-7977731-8, doi:10.2760/28321, JRC110486

Contents

Foreword

The Quality Assurance For Essential Climate Variable (QA4ECV) (FP7-607405) project aimed at developing a robust generic system for the Quality Assurance (QA) of satellite and in-situ algorithms and data records that can be applied to all Essential Climate Variables (ECVs) in a prototype for sustainable services in the frame of the Copernicus Climate Change Service (C3S).

The QA4ECV project also generated quality-assured multi-decadal Climate Data Records (CDR) for 3 atmospheric ECV precursors (nitrogen dioxide: NO2, Formaldehyde; HCHO, and Carbon Monoxide: CO) and 3 land ECVs (surface albedo, Leaf Area Index (LAI), and Fraction of Absorbed Photosynthetically Active Radiation (FAPAR), with full uncertainty metrics for every pixel ready for model ingestion.

The Joint Research Centre (JRC) retrieval algorithm was used to derive the Fraction of Absorbed Photosynthetically Active Radiation (FAPAR) from daily spectral measurements acquired by Advanced Very High Resolution Radiometer (AVHRR) onboard a series of National Oceanic and Atmospheric Administration (NOAA) platforms (Gobron, 2017). The inputs data were the surface Bidirectional Reflectance Factors (BRFs), derived from the normalised surface reflectances provided by the Land Long Term Data Record (LTDR) project (http://ltdr.nascom.nasa.gov, (Franch et al., 2017)).

The methodology itself was based on previous JRC-FAPAR algorithms such as the ones developed for the Medium Resolution Instrument Sensor (MERIS) and the Ocean Land Colour Instrument (OLCI), except surface reflectances instead of top of atmosphere ones are used as inputs. The uncertainty computations followed the main principles described into the Quality Assurance Framework For Earth Observation (QA4EO) guidelines (QA4EO, 2012), e.g. using the uncertainties propagation theory.

This report concerns the validation of the QA4ECV-FAPAR-AVHRR products through quality control at global scale from daily to 10-days and monthly period at $0.05^{\circ} \times 0.05^{\circ}$and $0.5^{\circ} \times 0.5^{\circ}$ spatial scale, with comparisons at local scale against other space products, *i.e.* LTDR AVHRR AVH15 (Claverie et al., 2016) and Two-stream Inversion Package (TIP) products (Pinty et al., 2011), using as inputs the MODIS Collection 6 surface albedo and 'green' a priori, and ground-based measurements.

Acknowledgements

This research has been supported by the EU FP7 Project Quality Assurance for Essential Climate Variables (QA4ECV), grant no. 607405.

Authors
Gobron N., Adams J., Lanconelli C., Marioni, M., Robustelli, M. and Vermote E.

Abstract

The Joint Research Centre (JRC) retrieval algorithm is used to derive the Fraction of Absorbed Photosynthetically Active Radiation (FAPAR) from daily spectral measurements acquired by Advanced Very High Resolution Radiometer (AVHRR) onboard a series of National Oceanic and Atmospheric Administration (NOAA) platforms (Gobron, 2017). The inputs data are the surface Bidirectional Reflectance Factors (BRFs), derived from the normalised surface reflectances provided by the Land Long Term Data Record (LTDR) project (http://ltdr.nascom.nasa.gov, (Franch et al., 2017)).

The methodology itself is based on previous JRC-FAPAR algorithms such as the ones developed for the Medium Resolution Instrument Sensor (MERIS) and the Ocean Land Colour Instrument (OLCI), except surface reflectances instead of top of atmosphere ones are used as inputs. The uncertainty computations follow the main principles described into the Quality Assurance Framework For Earth Observation (QA4EO) guidelines (QA4EO, 2012), e.g. using the uncertainties propagation theory.

This report concerns the validation of the QA4ECV-FAPAR-AVHRR products through quality control at global scale from daily to 10-days and monthly period at $0.05^\circ \times 0.05^\circ$and $0.5^\circ \times 0.5^\circ$ spatial scale, with comparisons at local scale against other space products, *i.e.* LTDR AVHRR AVH15 (Claverie et al., 2016) and Two-stream Inversion Package (TIP) products (Pinty et al., 2011), using as inputs the MODIS Collection 6 surface albedo and 'green' a priori, and ground-based measurements.

1 Introduction

The FAPAR is recognised as one of the fundamental Essential Climate Variable (ECV) by Global Terrestrial Observing System (GTOS) (Gobron and Verstraete, 2009) and Global Climate Observing System (GCOS) (GCOS, 2003, GCOS, 2016).

A series of JRC-FAPAR algorithms have been optimised for various optical instruments such as Sea-viewing Wide Field of View Sensor (SeaWiFS) (Gobron et al., 2002a), VEGETATION (Gobron et al., 2002c), GLobal Imager (GLI) (Gobron et al., 2002b), MERIS (Gobron et al., 2004, Gobron, 2011a), Moderate Resolution Imaging Spectroradiometer (MODIS) (Gobron et al., 2006b, Gobron et al., 2006a) and OLCI (Gobron, 2011b).

Validation exercises for the FAPAR values at medium spatial resolution scale have been performed for both SeaWiFS (Gobron et al., 2006c) and MERIS (Gobron et al., 2008).

In the context of QA4ECV Work Package (WP) 4, JRC generates daily FAPAR products at $0.05^\circ \times 0.05^\circ$; including its uncertainties from June 1981 to December 2006. From these daily products, both 10-days and monthly products are derived using time-composite algorithms. Furthermore regridding process provides dataset at $0.5^\circ \times 0.5^\circ$ for being used in global change studies.

The retrieval value aims to extract the 'green' FAPAR at the times of data acquisition in the plant canopy (and the angular rectified channels in the Band 1 and Band 2) from various NOAA platforms.

In this report, we first check the quality of the long time series over the QA4ECV validation sites, defined in (Gobron et al., 2015), from 1982 to 2006 using monthly products. In addition 10-days products are plotted over 2003-2004 against the 16-days JRC TIP that are processed using MODIS surface albedo Collection 6 under 'green' foliage assumption (see (Pinty et al., 2011)). The 3D-RT model simulations over the virtual scenes provide information of the expected differences between diffuse and direct values.

Secondly, 'validation' is assessed through comparison against time-series of past in-situ data, together with LTDR AVHRR FAPAR products (Claverie et al., 2016) and Two-stream Inversion Package (TIP) (Pinty et al., 2011) using as inputs the MODIS Collection 6 surface albedo and 'green' a priori. The overall results are discussed versus the source of problem using results from D3.7 (Lanconelli et al., 2017). The comparison between Earth Observation (EO) products and ground-based estimations of FAPAR is presented using the same categorisation of the ground-based FAPAR datasets according to their most probable radiative transfer regimes as already done in (Gobron et al., 2006c).

Thirdly, global 10-days products are compared against SeaWiFS ones for two years, *i.e.* 1999 and 2003 at $0.05^\circ \times 0.05^\circ$ as these two years correspond to AVHRR2 and AVHRR3 satellites, respectively. Both bias and Root Mean Square Deviation (RMSD) are reported together with AVHRR FAPAR uncertainties and the spatial standard deviation of SeaWiFS that are regridded from native spatial resolution, i.e. 1 km products. Note that such comparisons are done only over the 'best' grid-cells that are defined by minimising the cloud/cloud shadow occurrences in both products.

Finally, analysis of comparisons of monthly products at $0.5^\circ \times 0.5^\circ$ is then performed by assessing the averaged monthly bias to possibility create a long term bias corrected dataset.

2 Products overview

2.1 Definition

FAPAR results of multiple fluxes measurements balance within plant canopies.

'Total' FAPAR (absorbed component) comes from the energy balance between sources and sinks, with positive inputs corresponding to:

— Incoming PAR at the top of the canopy (direct and/or diffuse);

— Incoming PAR from propagating horizontally (mostly important at very high spatial resolution) ;

— Light reflected by the underlying ground (soil and/or understory)

and losses corresponding to:

— Outgoing PAR reflected by the canopy (top and bottom)

— Outgoing PAR propagating horizontally

Leaves-only FAPAR refers to the fraction of PAR radiation absorbed by live leaves only, i.e., contributing to the photosynthetic activity within leaf cells.

This quantity is lower than 'total' FAPAR because it does not include PAR absorption by the supporting woody material (in forest) or by dead leaves (in crops). This is illustrated in section 3.1 with the help of 3D-RT simulations over QA4ECV validation scenes.

2.2 Earth Observation

The space retrieval method used in QA4ECV project assumes that the leaves are alive and photosynthesizing, hence the name 'green' FAPAR.

It also means that the single scattering albedo of leaves is 'fixed' to only one value representing such 'green' leaves. This assumption is also used as 'a priori' when performing the TIP retrieval processing.

While FAPAR is typically based on an instantaneous measurement, for climate change applications representative daily values are required. They may be obtained through direct measurements, or by assuming variation with the cosine of the solar zenith angle to obtain the daily green FAPAR.

FAPAR products defined as a balance of multiple fluxes depends on the atmospheric conditions prevailing at the time of the measurements. In particular, estimates can be generated using direct, diffuse, or global radiation inputs. Knowledge on the type of incoming solar radiation fluxes is essential to properly interpret the data.

Similarly FAPAR can also be angularly integrated or instantaneous (i.e., at the actual sun position of measurement). As is the case for the surface albedo, one can define FAPAR estimates for a variety of atmospheric conditions and integrated in angles, space and times as needed.

QA4ECV FAPAR refers here to the instantaneous, *i.e.* black-sky, and green definition.

The theoretical FAPAR, values used in optimisation procedure are computed using the closure of the energy balance inside the plant canopy in the spectral range 400 to 700 nm (see (Gobron, 2017).)

TIP-FAPAR refers to the diffuse, *i.e.* white-sky, and green definition.

The FAPAR of the LTDR products, noted AVH15, is based on artificial neural networks (NN) calibrated using the MODIS FAPAR dataset (Claverie et al., 2016). The main algorithm is based on lookup tables (LUT) simulated from a 3-D radiative transfer model (Knyazikhin et al., 1998). The output is the mean FAPAR values computed over the set of acceptable LUT elements for which simulated and MODIS surface reflectances agree within specified level of (model and measurement) uncertainties. This NN is optimised over 6 land cover classes and no FAPAR values retrieval over bare or very sparsely vegetated area.

AVH15-FAPAR refers to the direct, *i.e.* black-sky, at local noon and polychrome definition.

2.3 Ground-based products

Past significant efforts were devoted to the validation of surface products such as FAPAR generated from data acquired by MODIS (Huemmrich et al., 2005, Wang et al., 2004, Shabanov et al., 2003). Ground-based FAPAR products correspond to physical quantities that can be measured in the field with different but significant levels of difficulty.

Impacts of different types of internal variability of the extinction coefficient together with the resolution of the sampled domain on the radiation transfer regime for clouds was analyzed by (Davis and Marshak, 2004) and they established the conditions where 3-D effects are anticipated to play a major role in the establishment of the radiation transfer regime. (Gobron et al., 2006c) extrapolated their results to the case of land surfaces by associating the main radiative transfer regimes against statistical properties of the leaf extinction coefficient inside the spatial domain of investigation. Therefore, the 'fast' variability regime is associated in the case of statistically homogeneous, Poisson-like, distributions of the leaf density, the 'slow' variability regime where the leaf density distribution (LAD) is close enough to being homogeneous only locally such that local scale average flux values are meaningful and the 'resonant' regime in other cases where the spatial complexity is such that a typical photon beam samples various types of structures between entering and escaping the canopy. Table 1 summarises the approach to assess the FAPAR value over the different sites used in this report and Table 2 the geolocation of field site together with their categorisation and land cover type.

Table 1: Ground-based measurements types

Field site Identification	Summary of the approach for domain-averaged FAPAR estimations
SN-Dhr	based on BBL's law with measurements of the LAD function
SN-Tes	FAPAR(μ_0) derived from the balance between the vertical fluxes
	$\langle LAI \rangle$ derived from PCA-LICOR
US-Seg	based on BBL's law with an extinction coefficient equal to 0.5[a]
	$\langle LAI \rangle$ derived from specific leaf area data and harvested above ground biomass
	advanced procedure to account for spatio-temporal changes of local LAI
US-Bo1	based on BBL's law with an extinction coefficient equal to 0.5[a]
	$\langle LAI \rangle$ from leaf area per plant area and plant density
	advanced procedure to account for spatio-temporal changes of local LAI
US-Ha1	based on BBL's law with an extinction coefficient equal to 0.58[a]
	$\langle LAI \rangle$ derived from optical PCA-LICOR data
	advanced procedure to account for spatio-temporal changes of local LAI
BE-Bra	based on full 1-D radiation transfer models
	$\langle LAI \rangle$ derived from optical PCA-LICOR data
	time-dependent linear mixing procedure weighted by species composition
US-Kon	based on BBL's law with an extinction coefficient equal to 0.5[a]
	$\langle LAI \rangle$ derived from optical PCA-LICOR data
	advanced procedure to account for spatio-temporal changes of local LAI
US-Me5	based on BBL's law with an extinction coefficient equal to 0.5[a]
	$\langle LAI \rangle$ derived from optical PCA-LICOR data
	advanced procedure to account for spatio-temporal changes of local LAI
ZM-Mkt	based on FIPAR estimated from TRAC data
	slight contamination by the woody canopy elements

a taken as constant, *i.e.*, independent of the Sun zenith angle.

Table 2: Anticipated radiation regime[(a)] of field sites

1 'Fast variability' Short and homogeneous over 1-2 km	2 'Slow variability' Mixed vegetation with different land cover types	3 'Resonant variability' Intermediate height and low density
SN-Dhr [(b)] semi-arid grass savannah	US-Bo1[(c)] corn and soybean	US-Me5[(c)] dry needle-leaf forest
SN-Tes[(b)] semi-arid grass savannah	US-Ha1[(c)] conifer/broad-leaf forest	ZM-Mkt[(e)] shrub-land/woodland
US-Seg[(c)] desert grassland	BE-Bra[(d)] conifer/broad-leaf/shrub forests	
	US-Kon[(c)] grassland/shrub-land/cropland	

a Based on (Davis and Marshak, 2004)'s analysis.
b See (Fensholt et al., 2004).
c See (Turner et al., 2004).
d See (Gond et al., 1999).
e See (Huemmrich et al., 2005).

3 Quality control of FAPAR time series over the QA4ECV validation sites

QA4ECV FAPAR retrieval is designed separately for each NOAA platform from 07 to 16 taken into consideration their own spectral responses in both Band 1 and Band 2. We therefore expect to have no drift into the time series of FAPAR, except the inter-seasonal and inter-annual variations over vegetated canopies. Of course, inputs data impact the output products quality and uncertainty. The following sub-sections discuss the FAPAR results over the QA4ECV birch and pine forests, tropical forests, crops and shrub/savannah sites, respectively. The green (red) dotted symbol indicates the best composite value in the case of clear-sky (LTDR cloudy) pixel. Grey shaded bar is the daily uncertainty of representative day and the error bar represents the standard deviation during the temporal period.

3.1 Background: FAPAR over QA4ECV scenes

Table 3 summarises the geolocation and land cover type of the QA4ECV validation sites over which the results are presented. Figures 1 to 4 illustrate the range values depending on various FAPAR definitions. The left hand side panels show the 'foliage' absorption as function of AVHRR sun zenith angle (dotted symbols) in 2003 and under diffuse radiation condition (dashed line) for the scenes used over validation sites. The right hand side panels illustrate the same but for the total component. One must notice that the seasonality, in the figures 1 to 4, is not the actual one but the DHR-FAPAR variation as function of the local sun zenith angle at the acquisition time. Each colour correspond to a virtual scene used in the simulations. The black diamonds indicate the value of current sun zenith angle for the AVHRR acquisition. These results are mainly used to discuss results in the next sections.

Table 3: QA4ECV Validation Sites

Site	Latitude (°N+)	Longitude (°E+)	Land Cover
Jarvselja-1	58.313	27.297	Birch Stand
Jarvselja-2	58.277	27.296	Pine Stand
Ofenpass	46.663	10.230	Pine Stand
Lope	-0.169	11.459	Tropical Forest
Nghotto	3.867	17.300	Tropical Forest
Zerbolo	45.295	8.877	Short Rotation Forest (Poplar)
Thiverval-Grignon	48.85	1.966	Wheat
Wellington	-33.600	18.933	Citrus Orchard
Skukuza	-25.0197	31.4969	Savannah
Libya4	28.55	23.39	Desert
Janina	-30.077	144.136	Shrub land
Dome-C	-75.100	123.300	Snow

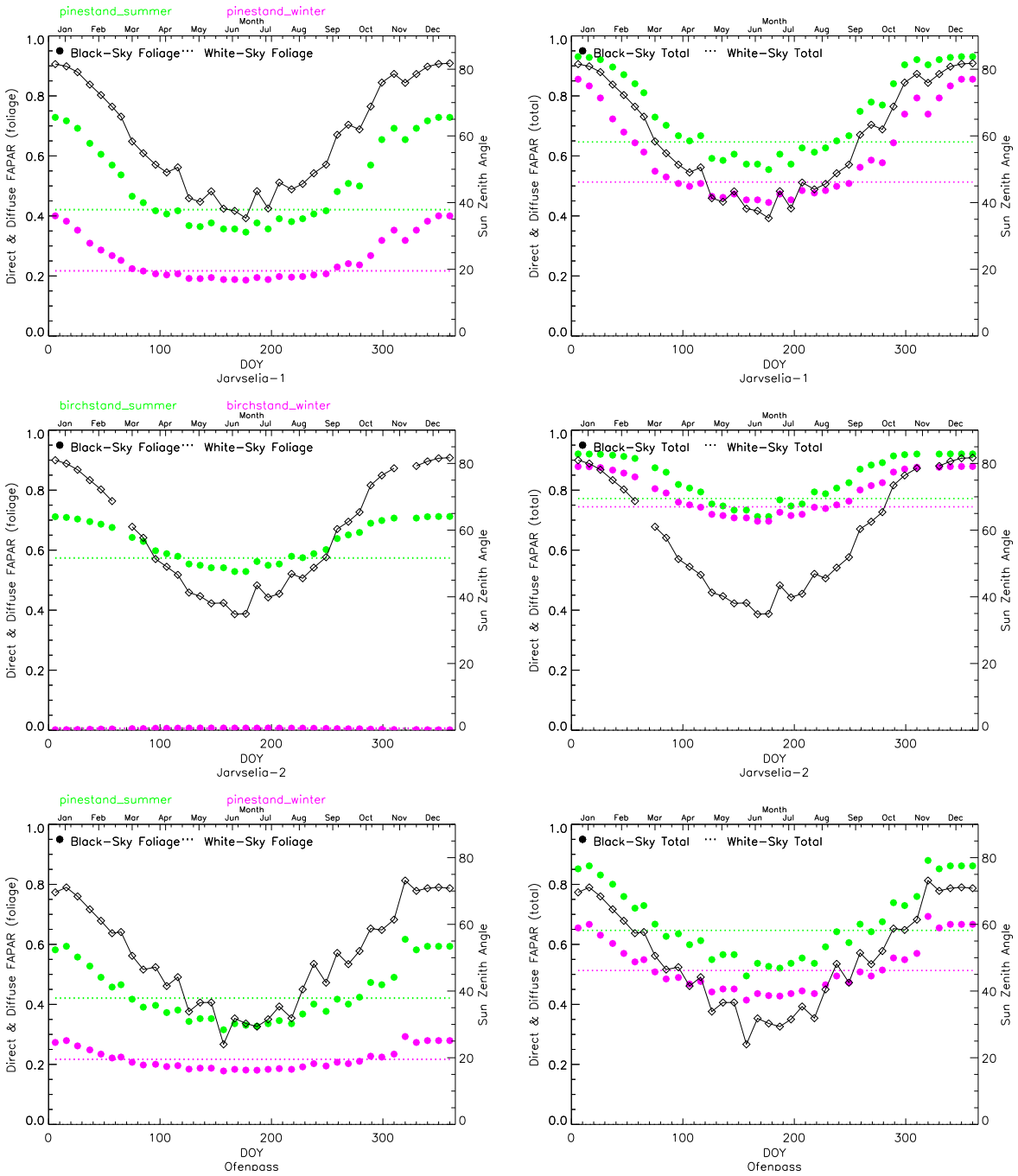

Figure 1: Time series of diffuse and direct FAPAR over QA4ECV forest sites using actual sun zenith angles of AVHRR. Left and right hand side panels correspond to foliage and total component, respectively.

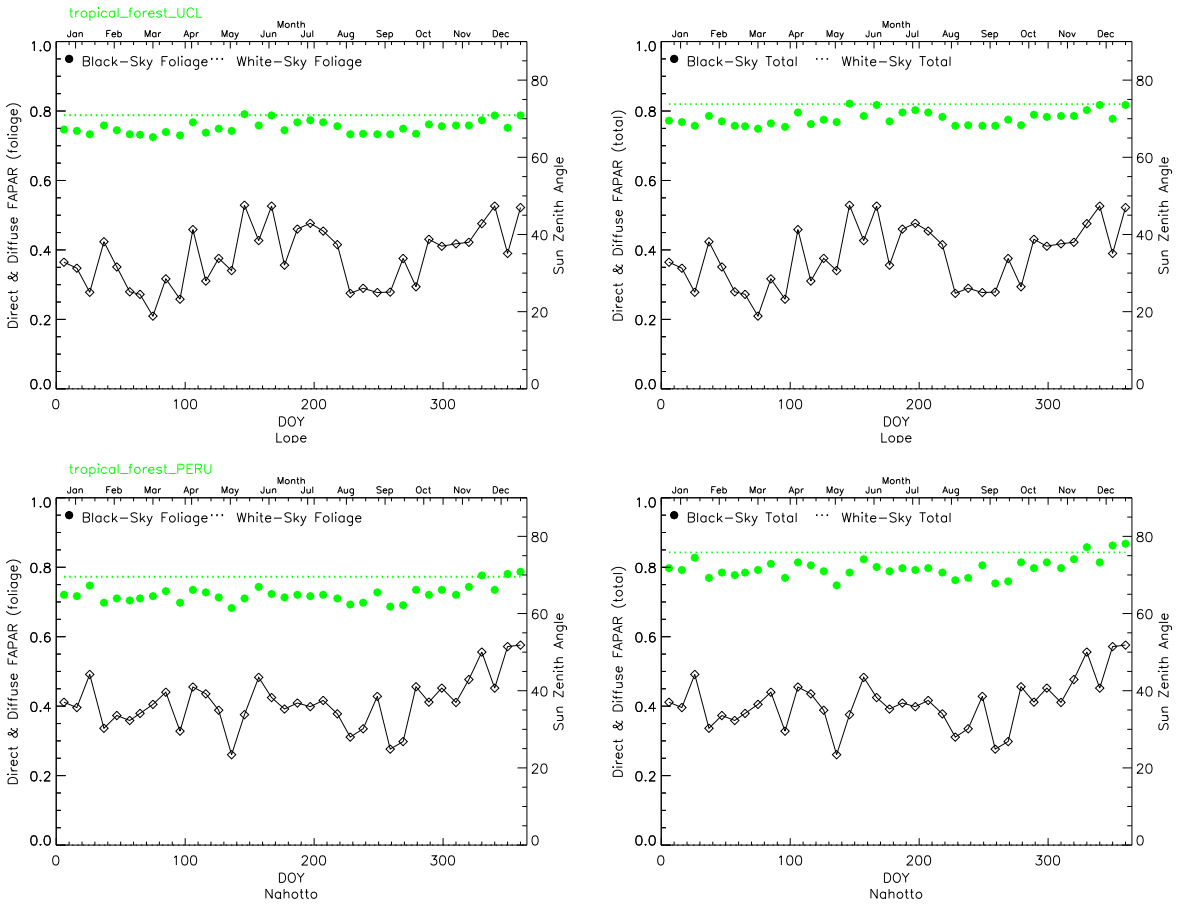

Figure 2: Same as Figure 1 but over QA4ECV tropical forest sites.

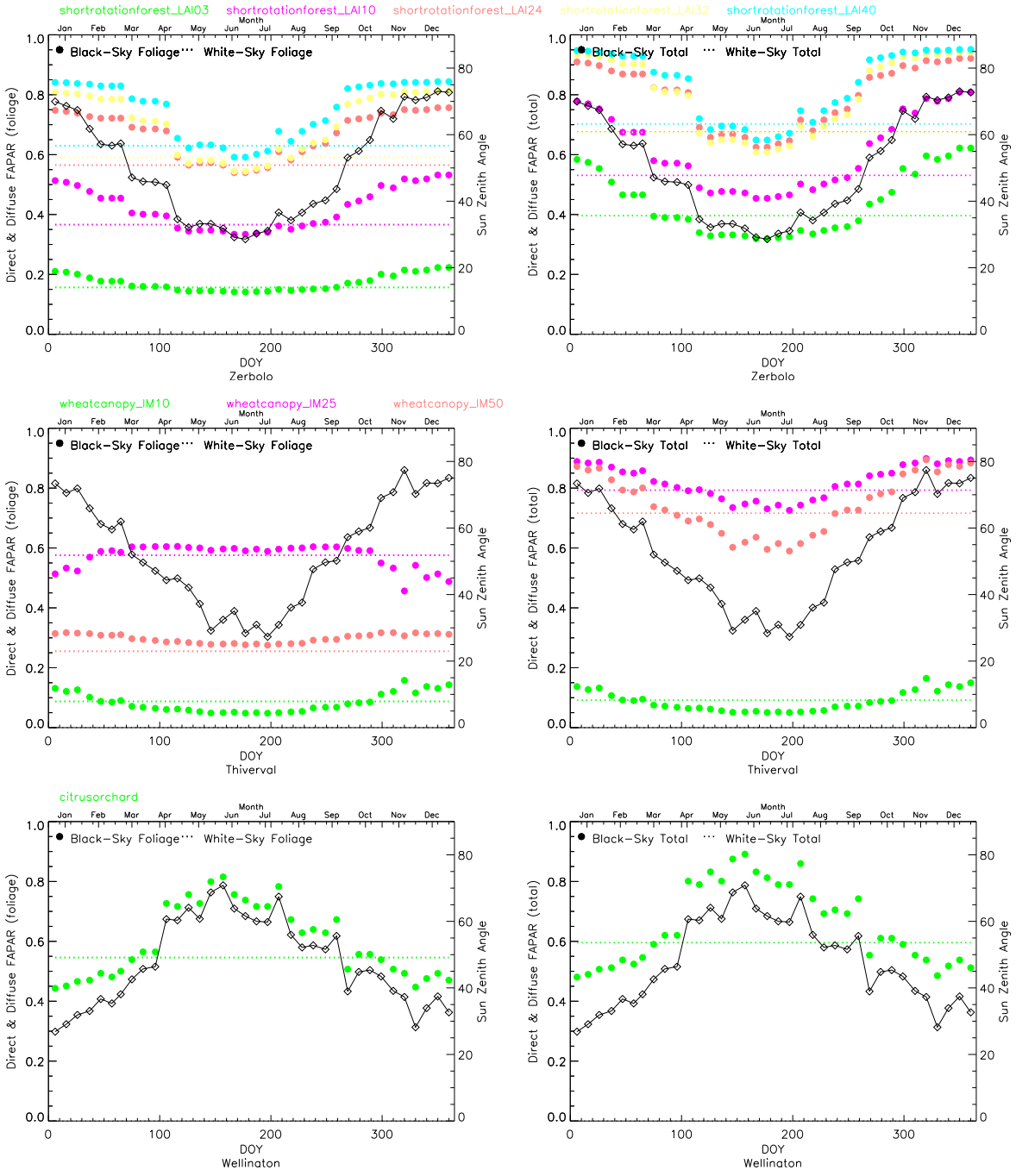

Figure 3: Same as Figure 1 but over QA4ECV crops sites.

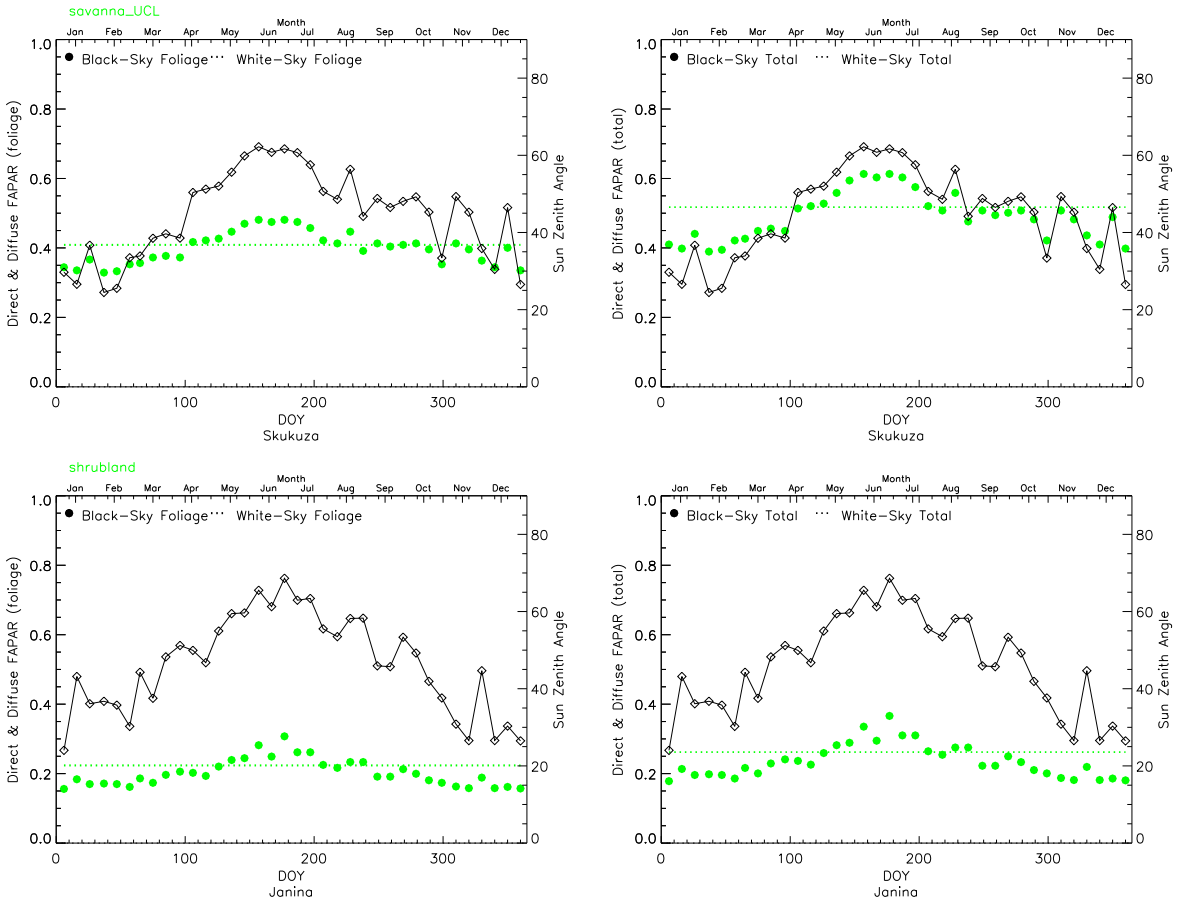

Figure 4: Same as Figure 1 but over QA4ECV shrub and savanna sites.

3.2 Monthly time series over 1982-2006

The following section presents the time series of monthly AVHRR FAPAR products at $0.05° \times 0.05°$ over the QA4ECV validation sites. The following subsections present results in accordance to each land cover type.

3.2.1 Birch stand and pine stand forest sites

The birch stand/pine stand forests sites results are plotted in Figure 5. Green (pink) circle symbols correspond to FAPAR best representative value that are not affected by cloud during each month over vegetation (soil). Red circle symbols indicate LTDR cloud flag meaning that no clear sky days were found during the time composite period.

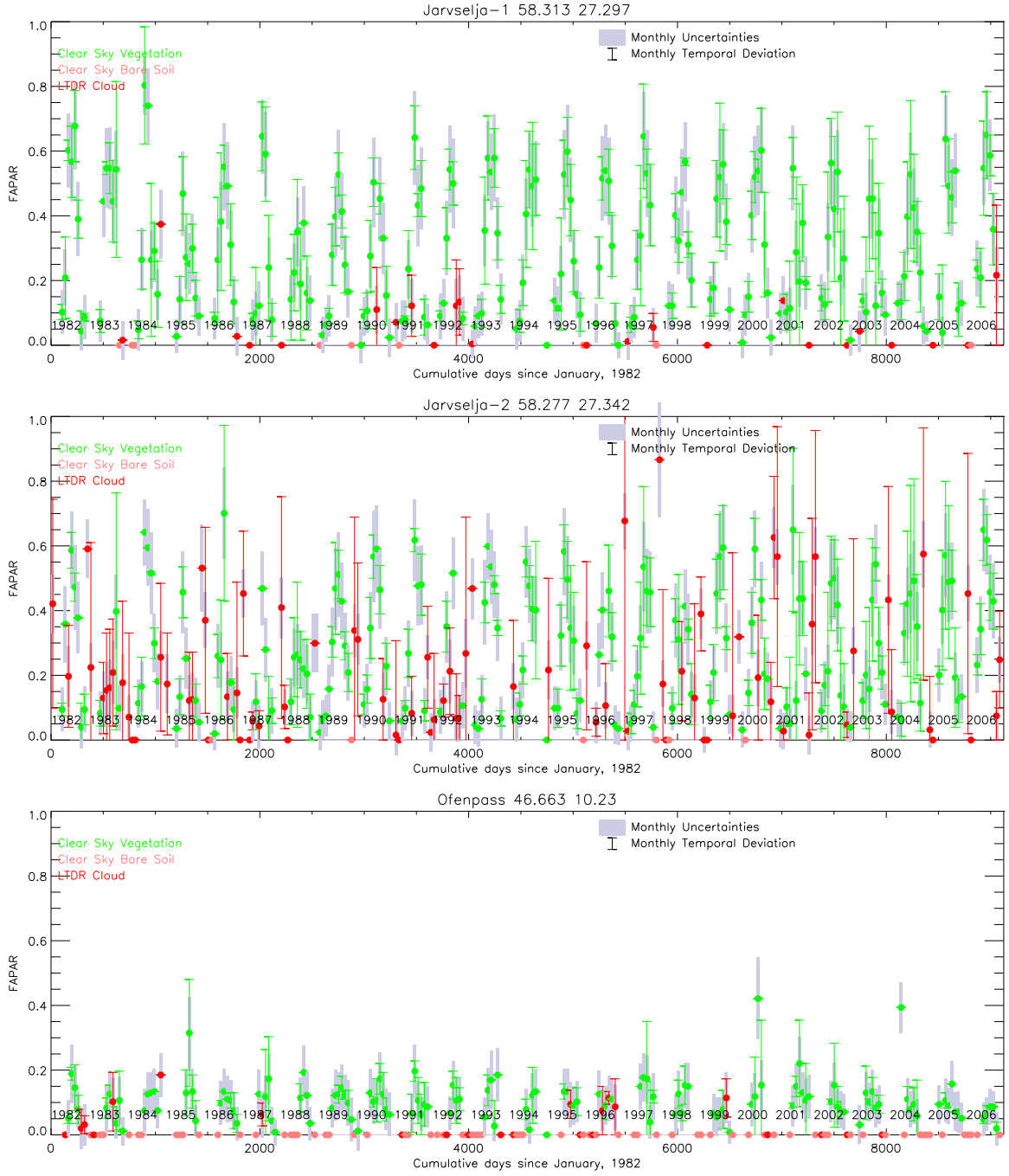

Figure 5: Time series of monthly FAPAR products over QA4ECV forest sites

The shade bars indicate the uncertainties of this best day whereas the error bars represent the temporal standard deviations during a month. The inter-annual seasonalities over 1982 and 2006 are in general well represented expect over few months for which outliers are detected. The level over Ofenpass is very low comparing to Jarvselja-1 even so the same land cover, i.e. scene was assigned.

The theoretical range of FAPAR that is expected over pinestand summer (winter) virtual scene over Ofenpass varies from 0.3 (0.2) to 0.6 (0.3) depending on the sun zenith angles. Over Jarvselja-1 we have slightly higher values. Using actual EO data, we found rather a bigger differences which may be explained by a wrong scene associated to Ofenpass. During northern hemisphere winter seasons, bright surfaces are detected over this site so null FAPAR values. Over Jarvselja-2 monthly products still provide a lot of data contaminated by clouds, especially during winter seasons.

3.2.2 Tropical forest sites

The two tropical forest sites long time series are plotted in Figure 6. The values over Lope present lower FAPAR values comparing to Nghotto and their respective maxima are 0.4 and 0.6, which is lower comparing to 3D-RT model simulations (see Figure 2). However, (Lanconelli et al., 2017) show that when the retrieval algorithm is applied to simulated surface reflectance results are much higher than with real data: this means that atmospheric correction may suffer from clouds contamination at the 0.05°× 0.05° as it is often the case over these tropical regions.

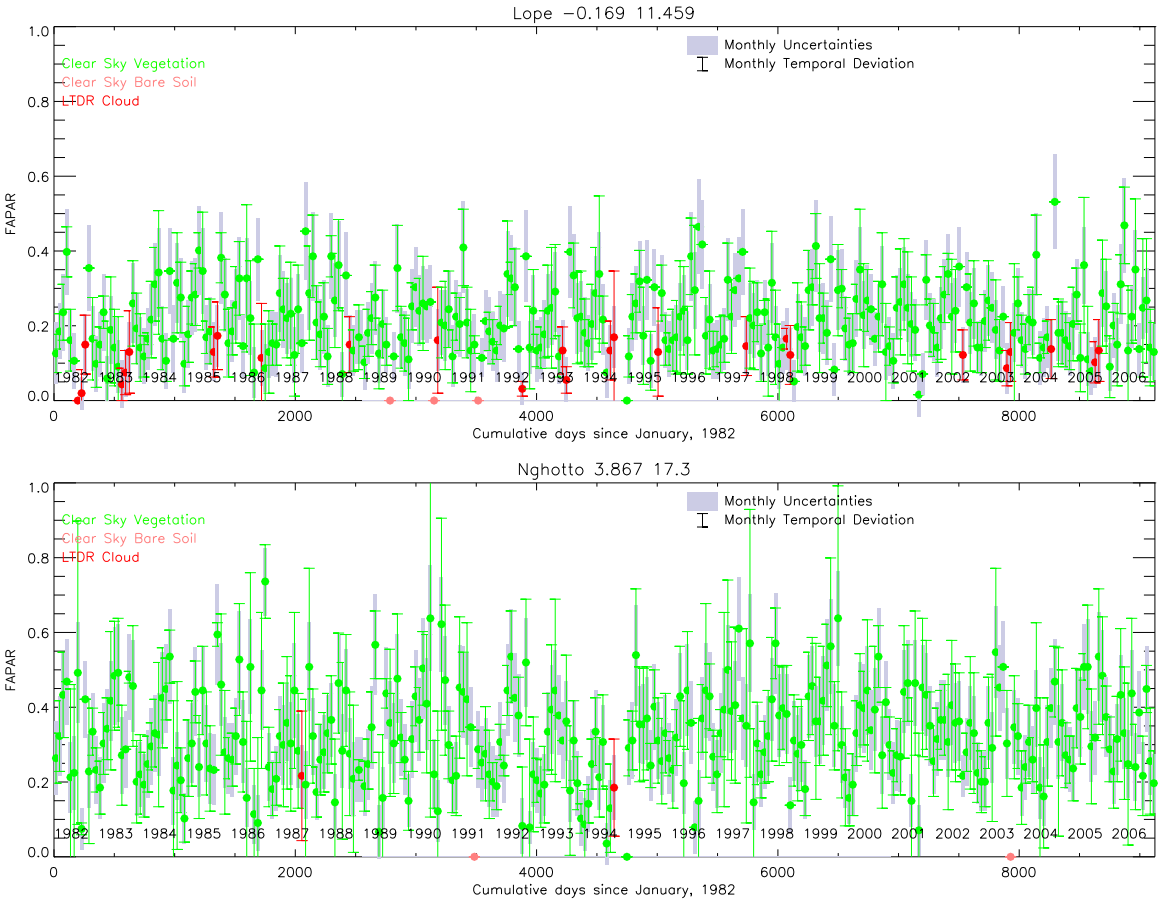

Figure 6: Time series of monthly FAPAR products over QA4ECV tropical forest sites

3.2.3 Crops sites

FAPAR time series over three different types of crops are plotted in Figure 7. The top panel shows short rotation poplar forest over Zerbolo site. The middle and bottom panels correspond to wheat and citrus orchard crops, respectively. Over this latter site, few outliers appear: one in 1998 and various in 1994 when inputs data suffer from three month of missing data and artefacts in south hemisphere. One can notice that the products represent very well the expected seasonality over crops each year with high level during summer at about 0.7 over Zerbolo.

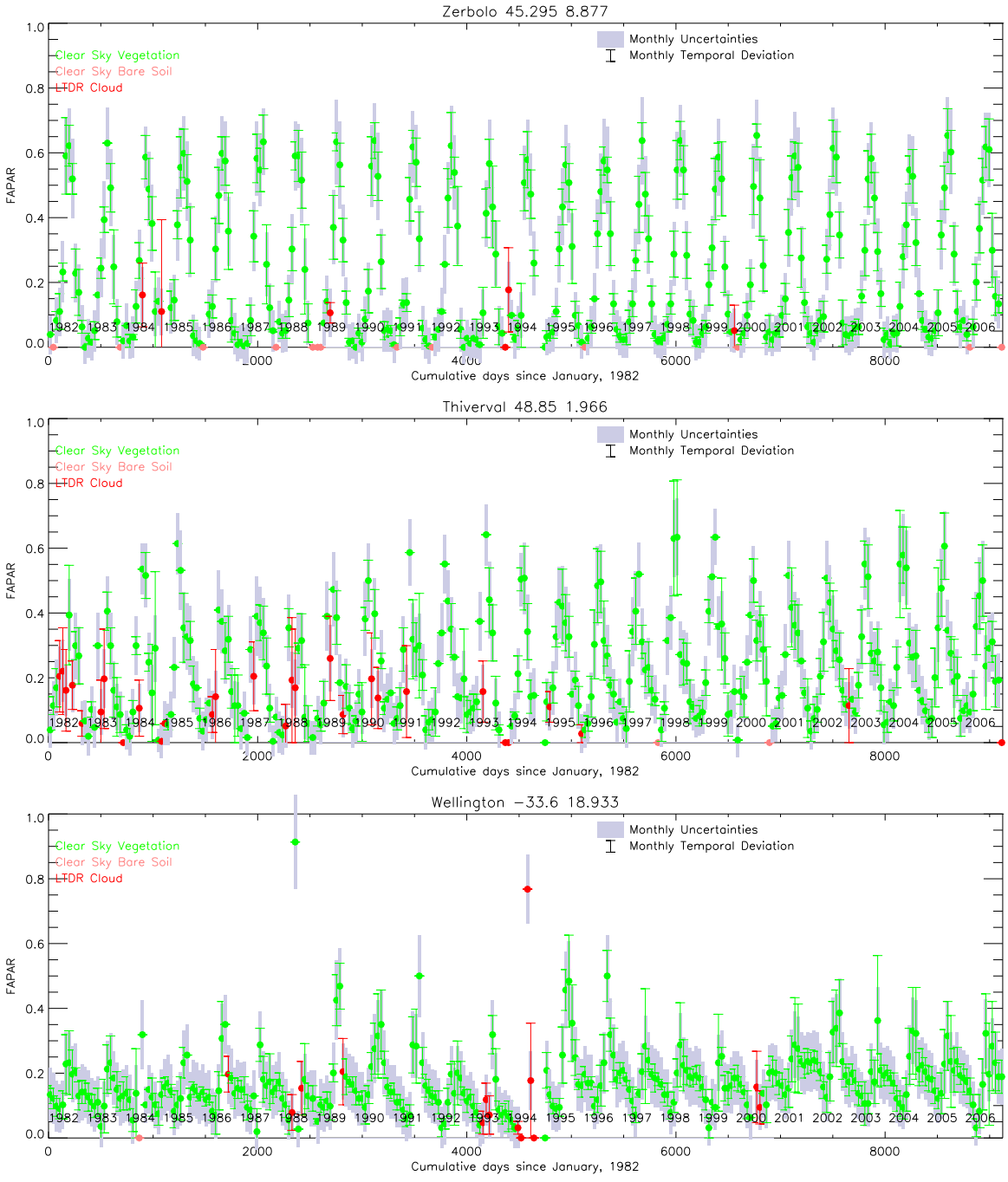

Figure 7: Time series of monthly FAPAR products over QA4ECV crops sites

3.2.4 Shrub and Savanna sites

FAPAR time series over shrub and savanna sites are displayed in Figure 8. The top panel reports the results over Skukuza site whereas the bottom one shows the shrub land FAPAR evolution over Janina site. Over both sites, few outliers appear in the three month of missing data and artefacts in 1994 for which only one day of results is available (indicating by the absence of error bar). The overall seasonality of both vegetation are well represented during the entire long period.

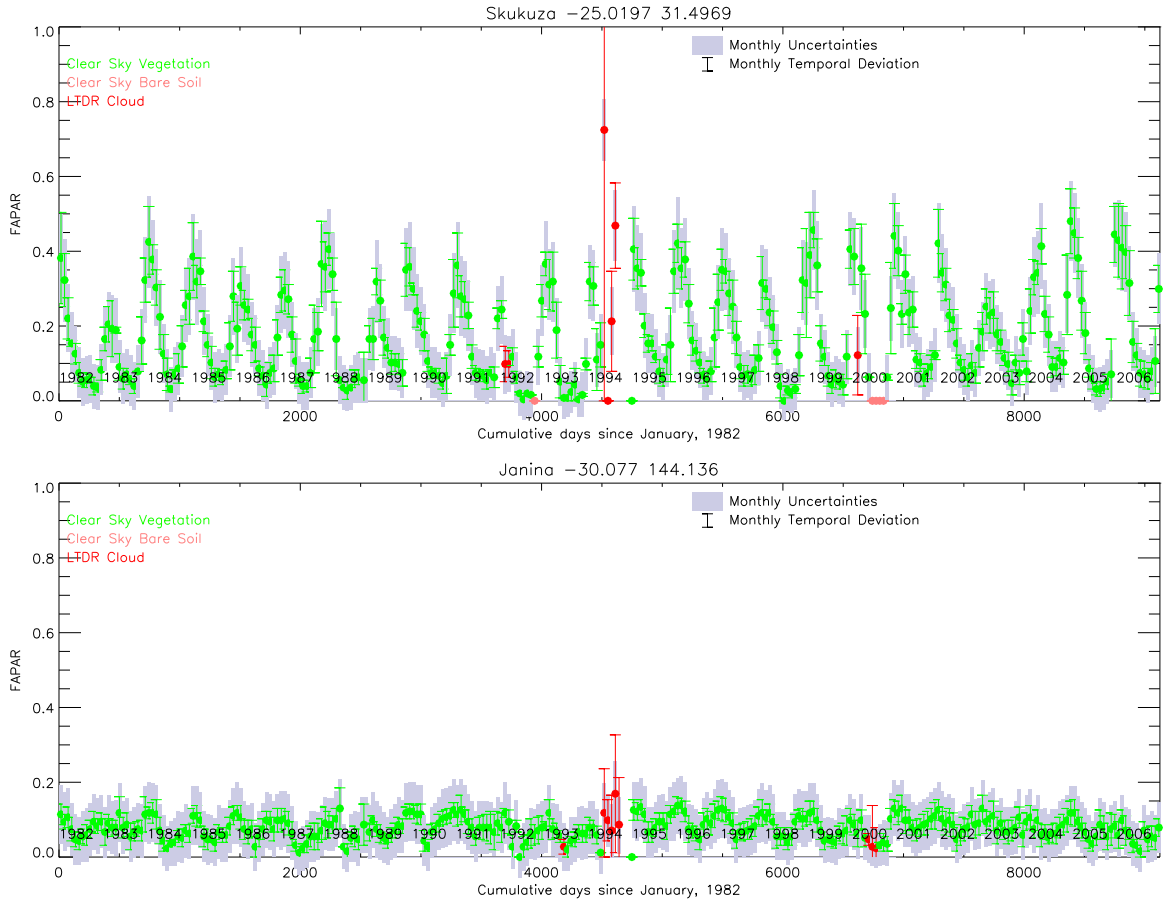

Figure 8: Time series of monthly FAPAR products over QA4ECV shrub and savanna sites

3.3 Two years of 10-days and TIP comparisons

This section shows the 10-days QAECV AVHRR FAPAR over 2003-2004 period together with the 16-days JRC TIP FAPAR at 1 km derived from MODIS albedo Collection 6. As already mentioned, QA4ECV AVHRR FAPAR values correspond to direct absorption of 'green' foliage, meaning that the FAPAR values depend on the actual sun zenith angle, whereas the TIP values provide the diffuse FAPAR values. The expected differences, from a theoretical point of view, are assessed using the 3D-RT model simulations as function of the day of the year over each site using respective 3D scene(s) from Figure 1 to Figure 4.

3.3.1 Birch stand and pine stand forest sites

Three panels in Figure 9 illustrate two years of 10-days AVHRR and 16-days JRC TIP FAPAR over Jarvselja-1, Jarvselja-2 and Ofenpass sites, respectively. Dotted green dots represent the QA4ECV results with error bar for the temporal standard deviation during the 10-days period and uncertainty with shade grey colour.

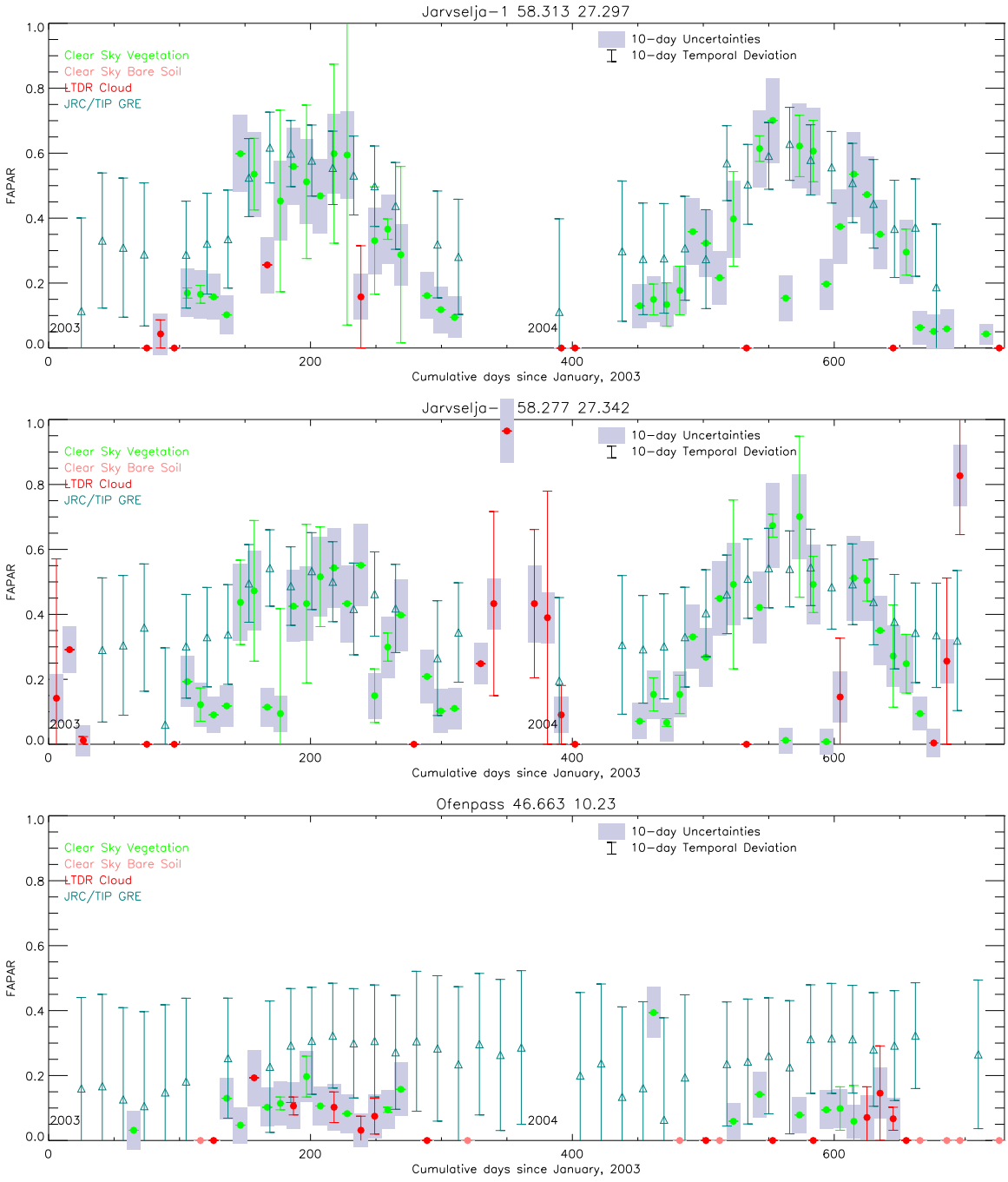

Figure 9: Time series of 10-days FAPAR products over QA4ECV forest sites with JRC TIP C6

When results are associated with a LTDR cloud mask, the formers are plotted in red colour. Bar soil flag are displayed in pink colour. JRC TIP are over-plotted in blue colour triangle symbols. During summer months the results between the two land algorithms agree well over the three forest canopies but are slightly different over Ofenpass site for which AVHRR FAPAR provide lower values: this can be due to the difference between diffuse and direct values as shown in bottom panel in Figure 1. During winter months, there is no result provided by AVHRR or un-trustable due to cloud/snow contamination contrary to TIP as this retrieval algorithm can assume a prior snow background.

3.3.2 Tropical forest sites

Two panels in Figure 10 illustrate the 10-days AVHRR and 16-days JRC TIP FAPAR over tropical forest sites over 2003-2004. Dotted green dots represent the QA4ECV results with error bar for the temporal standard deviation during the 10-days period and uncertainty with shade grey colour.

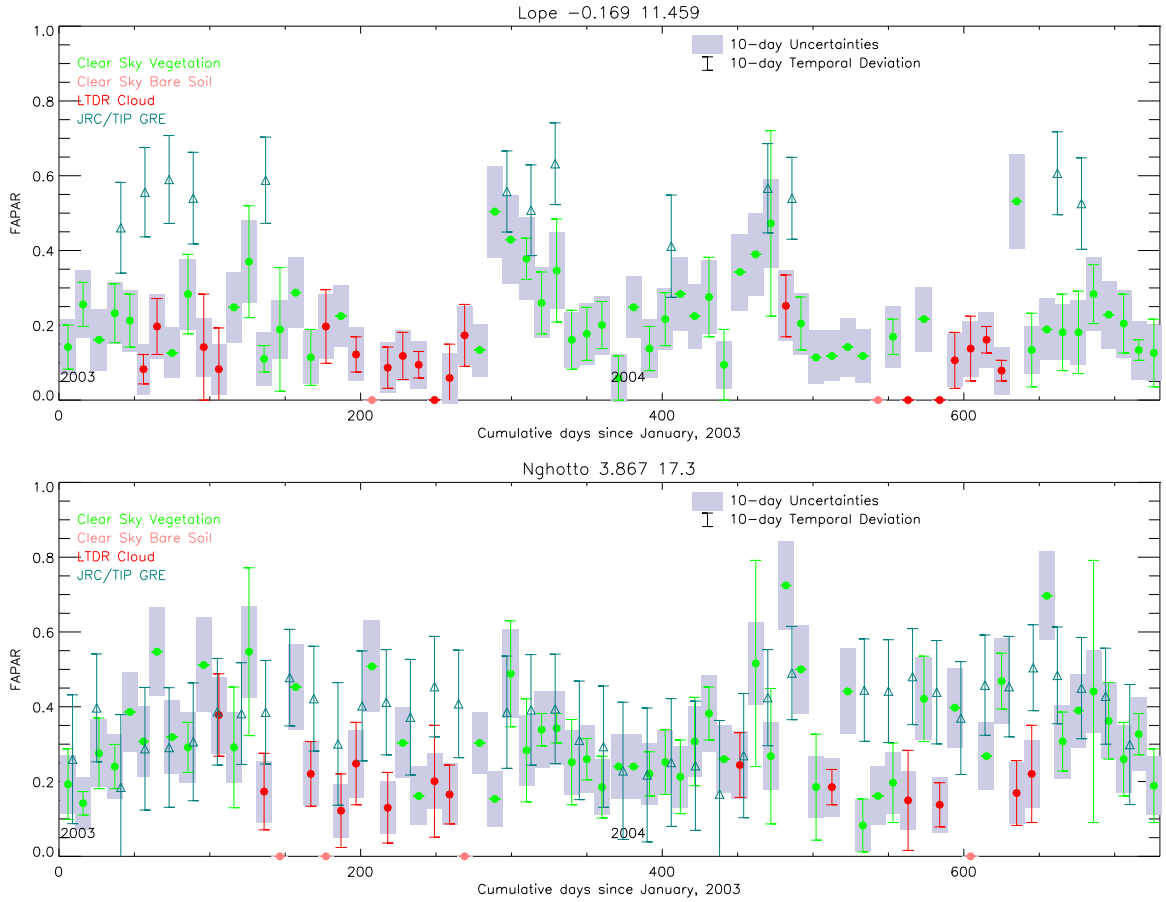

Figure 10: Time series of 10-days FAPAR products over tropical forest sites with JRC TIP C6

When results are associated with a LTDR cloud mask, the formers are plotted in red colour. Bar soil flag are displayed in pink colour. JRC TIP are over-plotted in blue colour triangle symbols. Over Lope site, top panel, TIP retrieved less results than AVHRR ones that can be due to low level of quality in MODIS albedo due to recurrent cloud contamination over tropical zone. Its level is however high with value around 0.5 which is anyway lower than the expected theoretical values, *i.e.* 0.7, found in top panel of Figure 2. The values of direct FAPAR are low comparing to theoretical value which can be explained by the leaf single scattering albedo assumed in JRC algorithm. Over Nghotto site, bottom panel, the two products provide same amplitude variability except during summer months.

3.3.3 Crops sites

Figures 11 and 12 show the 10-days AVHRR and 16-days JRC TIP FAPAR over three crops sites over 2003-2004. Dotted green dots represent the QA4ECV results with error bar for the temporal standard deviation during the 10-days period and uncertainty with shade grey colour. When results are associated with a LTDR cloud mask, the formers are plotted in red colour. Bar soil flag are displayed in pink colour. JRC TIP are over-plotted in blue colour triangle symbols. Seasonality and amplitude of both products agree well with expected crop phenology over the three types of crop. Over Wellington site, covered by citrus orchard, TIP values are always higher. This maybe due to

the spatial scale difference of products as TIP is at 1 km and AVHRR at 0.5 °. One can notice higher seasonal variation with AVHRR products.

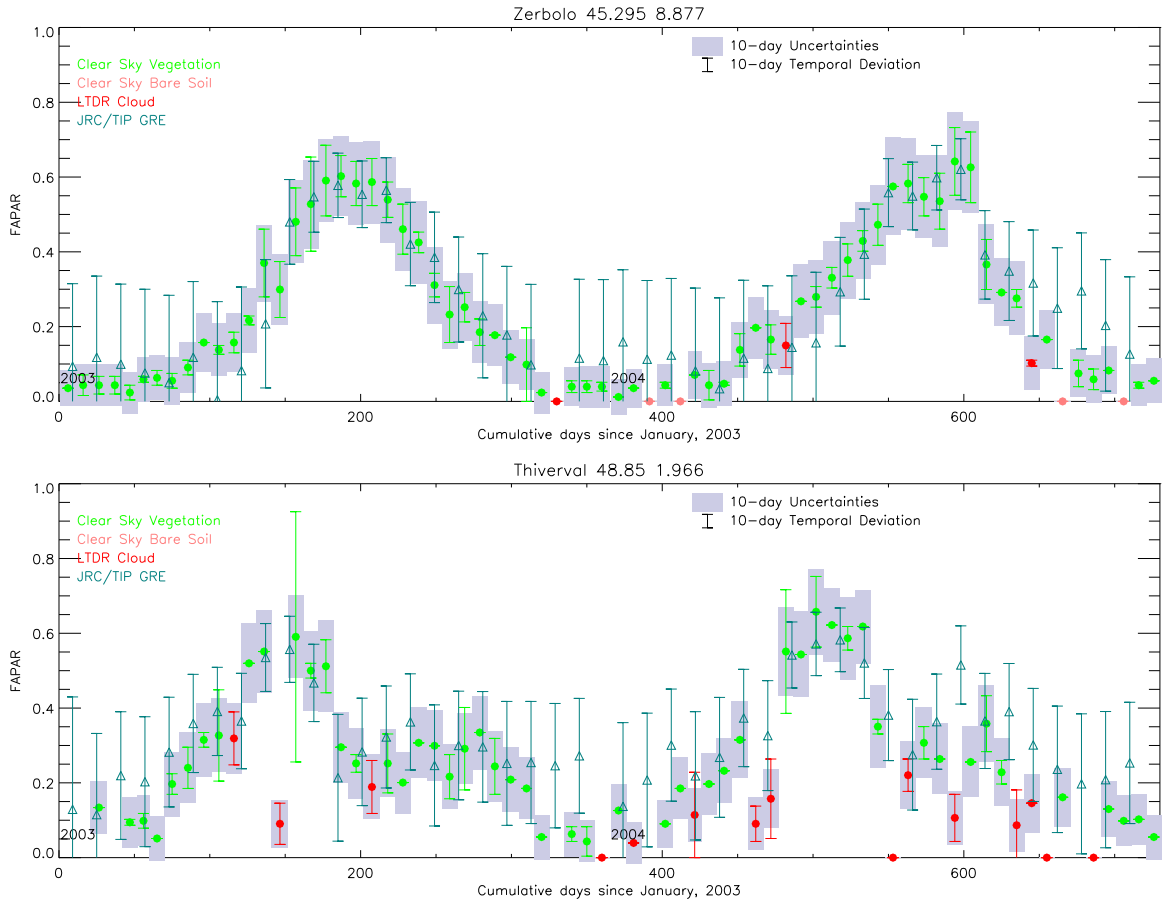

Figure 11: Time series of 10-days FAPAR products over two QA4ECV crops sites with JRC TIP C6

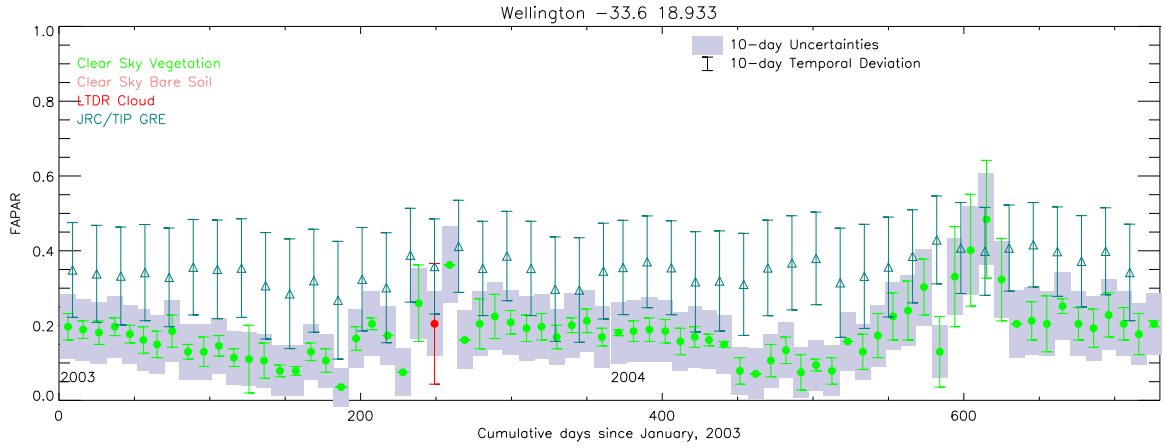

Figure 12: Time series of 10-days FAPAR products over QA4ECV Wellington site with JRC TIP C6

3.3.4 Savanna and shrub sites

Finally, both panels in Figure 13 show the 10-days AVHRR and 16-days JRC TIP FAPAR over Skukuza and Janina sites, respectively covered by savanna and shrub-land. Dotted green dots represent the QA4ECV results with error bar for the temporal standard deviation during the 10-days period and uncertainty with shade grey colour. The seasonalities of such canopies are well represented by both products with TIP values always higher than the AVHRR ones and in agreement with theoretical values. Here again spatial variability and assumption in the leaf single scattering albedo may be explain this difference.

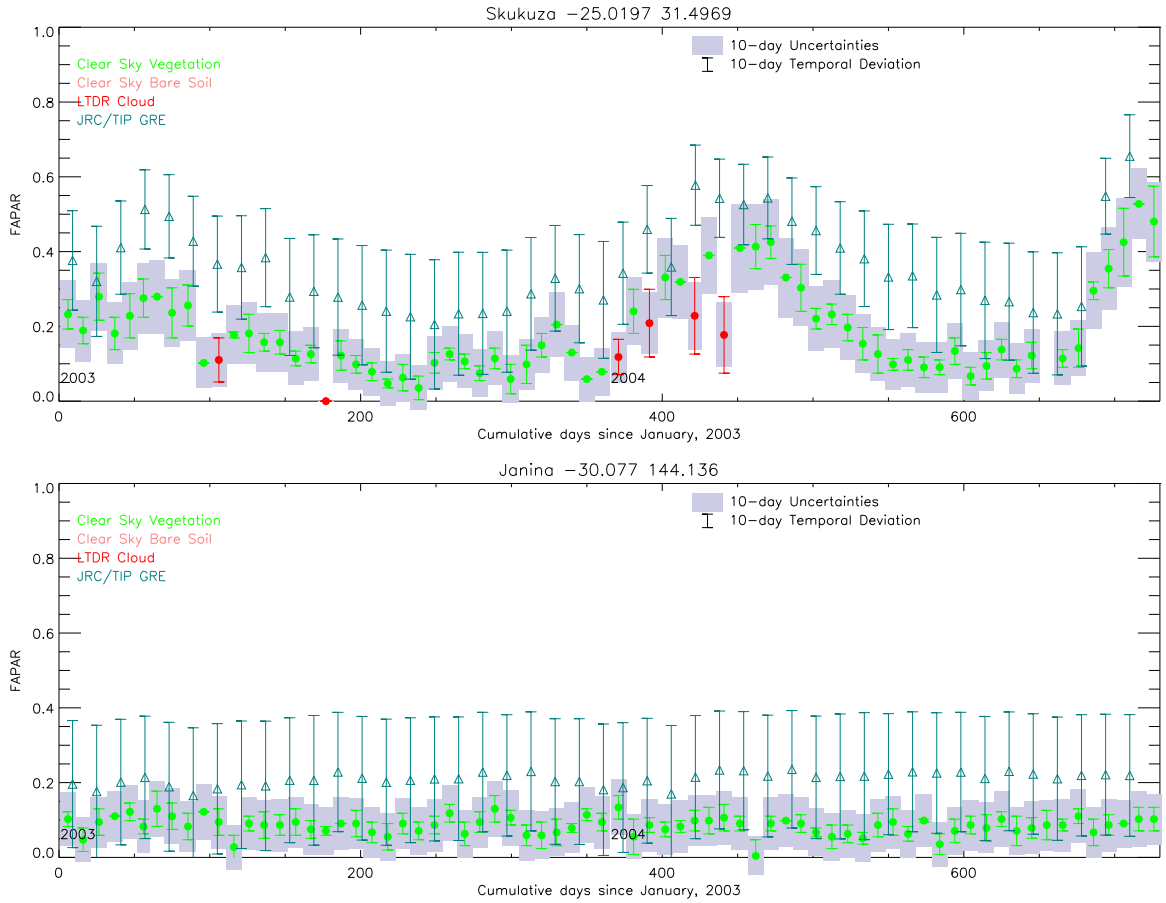

Figure 13: Time series of 10-days FAPAR products over QA4ECV shrub and savanna sites with JRC TIP C6

3.4 Quality control of rectified channels in Band 1 and Band 2 over CEOS validation site

The rectified channels are surface reflectances decontaminated from angular effects. Time stability of the signal is expected in both channels. Top and bottom panels of Figure 14 display Band 1 and Band 2 results, respectively. In both channels, we can see various issues at the end of 1984, 1887 and 2006 and at the beginning of 1989. There are few outliers that are presented at the same times in both channels and provide lower values comparing to averaged ones. These values come from daily inputs Top Of Atmosphere (TOA) artefacts that are propagated to the rectified channels.

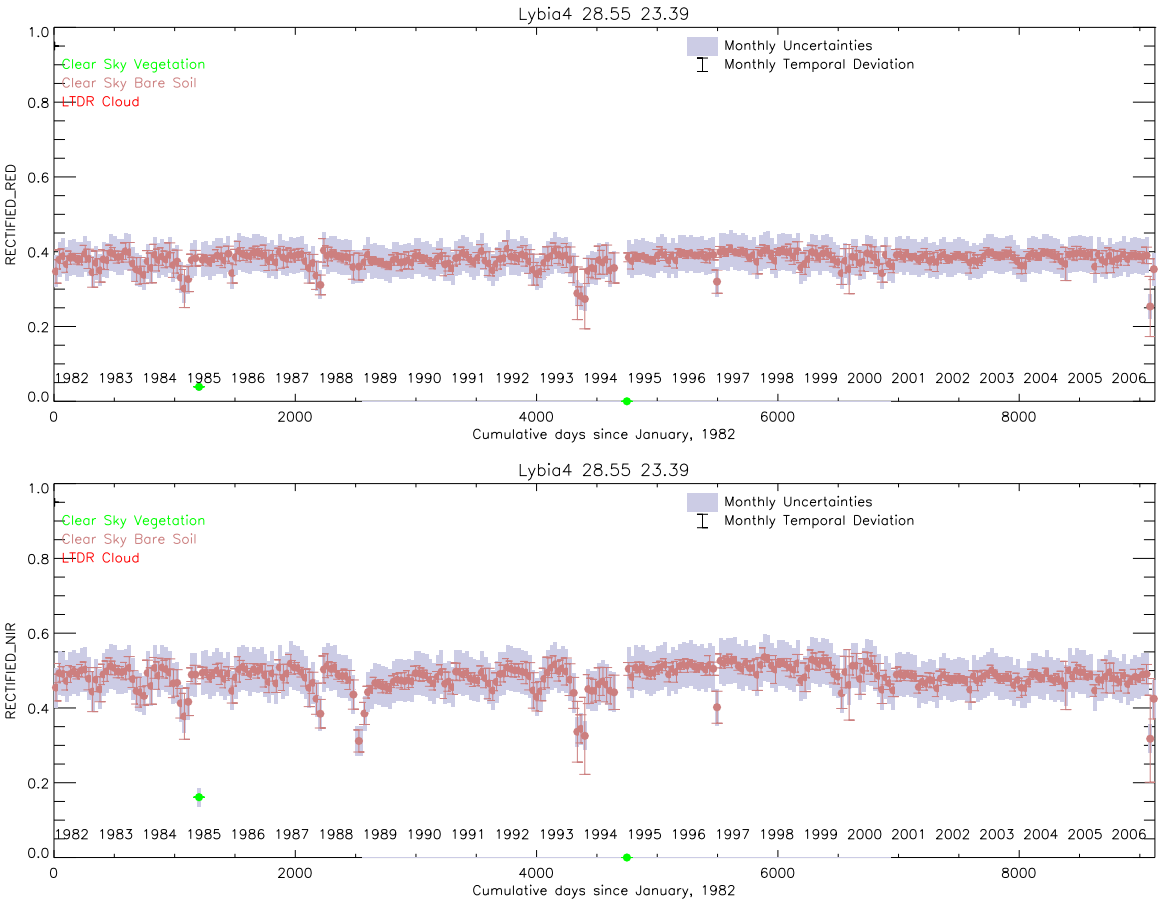

Figure 14: Time series of monthly Rectified Band 1 and Band 2 products over QA4ECV CEOS site

4 Validation using ground-based measurements

The QA4ECV FAPAR products are now compared against ground-based measurements already used in (Gobron et al., 2006c). Table 1 summarizes the ground-based methodology information. In addition, daily products that used the same surface reflectance data (Claverie et al., 2016) and 16-days TIP FAPAR green products using as inputs the MODIS albedo Collection 6 are plotted in green diamonds and blue triangle colour symbols, respectively.

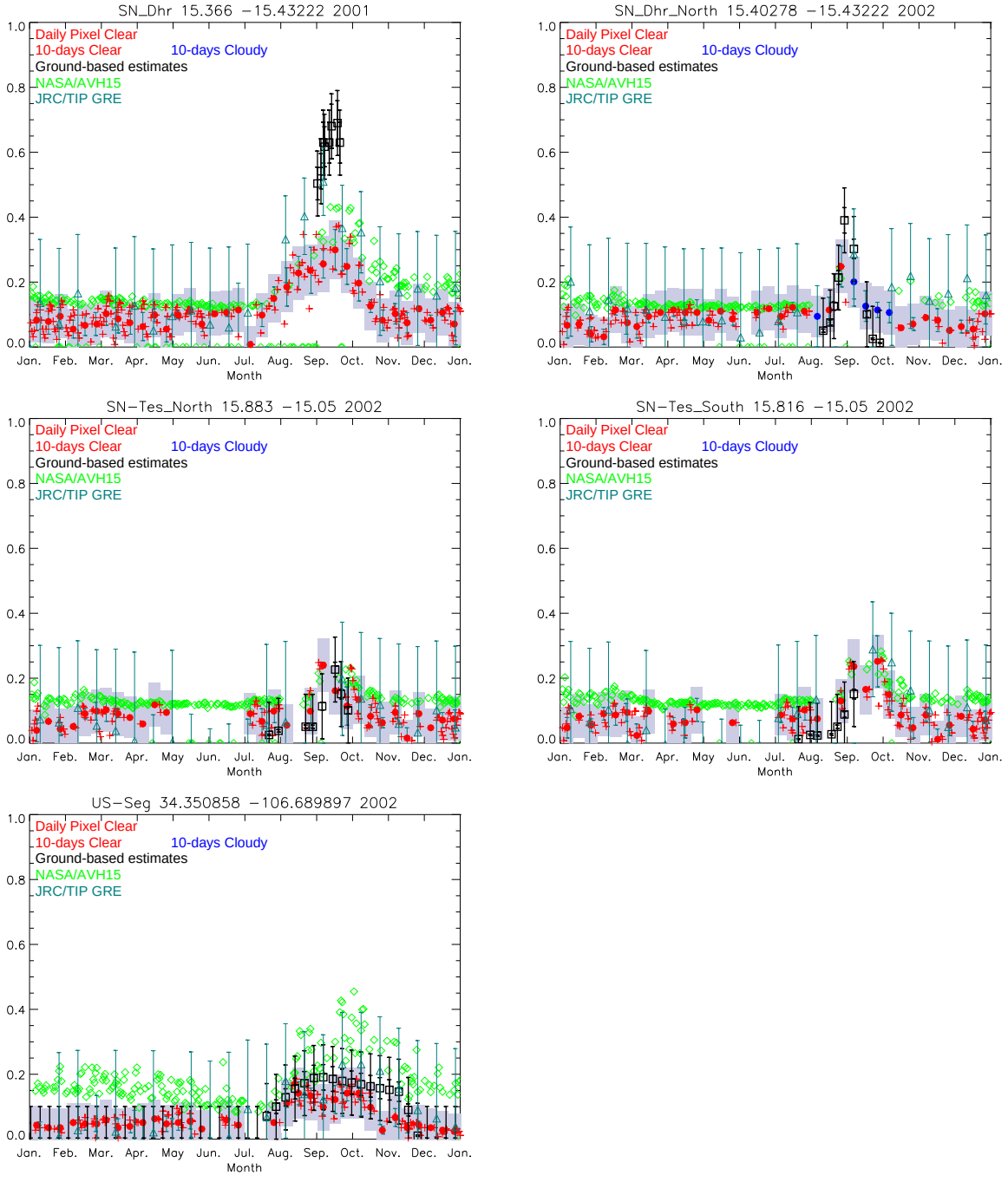

Figure 15: Time series associated with radiation transfer regime 1.

Figure 15 displays the time series of the space FAPAR products together with the ground-based estimations available from five sites, located in Senegal, *i.e.* SE-Dhr [15.366°N,-15.432°E]; SE-Dhr North [15.402°N,-15.432°E]; SN-Tes [15.883°N,-15.05°E] and SN-Tes South[15.816°N,-15.05°E], and in US over Sevilletta, US-Seg [34.35°N,-106.69°E], all associated with radiation transfer regime 1, corresponding to the so-called 'fast variability' category. The baseline FAPAR value over these sites is very low and signatures of the different vegetation phenological cycles (both for the growing and senescence periods) are remarkably well identified by both space and ground-based estimations.

Moreover, the amplitudes, both maxima and minima, are in very good agreement with all products although the space retrievals tend to slightly underestimate the ground-based values over the site

of SN-Dhr during the peak season for 2001 (top left hand side panel). Indeed, at this latter site the landscape exhibits significant spatial heterogeneity at mesoscale which was not sampled by the ground-based measurements (and thus was not accounted for in the FAPAR ground-based estimations) but which was probably captured at the resolution available from the satellite FAPAR products. AVH15 is slightly larger than both AVHRR and TIP products, specially over the desert-grassland (bottom panel). Both TIP and AVHRR FAPAR products agree well within their respective uncertainties.

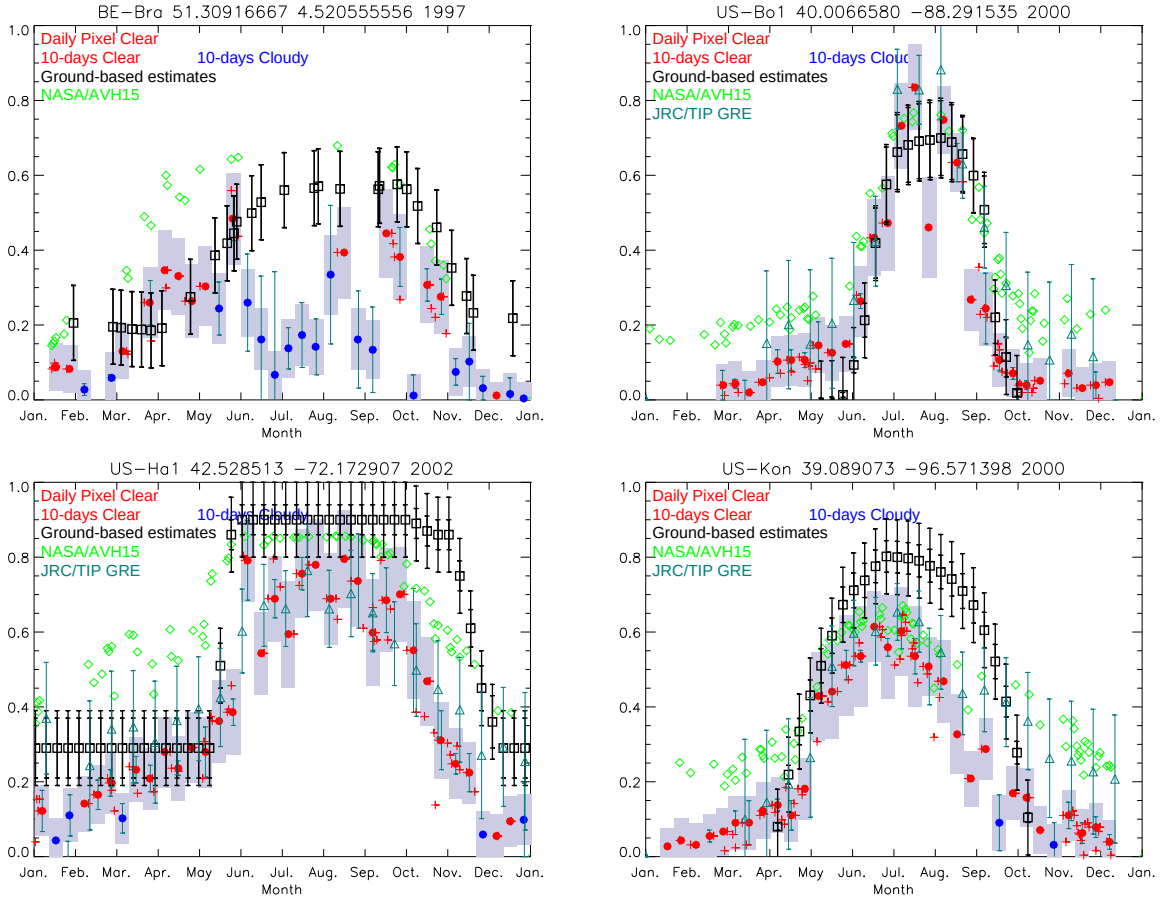

Figure 16: Time series associated with radiation transfer regime 2.

Results over vegetation conditions belonging to the 'slow variability' category, that is radiation transfer regime 2, are displayed in Figure 16. In the case of BE-Bra site [51.309°N,4.52°E] (top left hand side panel) the amplitudes in 1997 between the start and end of the growing season estimated from both remote sensing and ground measurements are in very good agreement. However QA4ECV results are suffering from cloud contaminations (blue dots) from June to August. The ground-based estimated FAPAR values over the agricultural field site identified as US-Bo1 [40.006°N,-88.291°E] follow a well-defined time trajectory that is correctly tracked by the QA4ECV FAPAR products (red dots) and JRC TIP (triangle) (top right panel of Figure 16). Daily AVH15 (green diamonds) reveal higher level than other measurements until June and after September. The third comparison performed with regime 2 canopy conditions, is conducted at the Harvard site (identified as US-Ha1) which is a mixture of conifer and hardwood forests. Results from TIP and QA4ECV data sets (bottom left hand side panel on Figure 16) compare very well with each other and ground-based measurements for the first 6 months of the year which includes the growing period. All space products then show systematically lower values than the ground-based estimations during the summer season where vegetation gets very dense over the site. The largest difference occur during the senescent period where a time delay of about 1 month is observed between the FAPAR signatures given by space and ground-based datasets. Both remote sensing and ground-based estimations of FAPAR over the US-Kon tallgrass prairie site [39.089°N, -96.571°E] indicate the occurrence of a well-marked vegetation seasonal cycle (bottom right hand side panel on Figure 16). JRC TIP and QA4ECV estimations are well correlated along the cycle over this site covered by mixed grassland/shrub land and cropland, although the JRC FAPAR products are slightly biased low. Such a bias occurring during the period of senescence is a consequence of using total (in ground-based estimations) instead of green (as assumed in the retrieval algorithm) values when assessing the FAPAR values as illustrated in Figure 3.

The comparison results of ground-based and space retrieved FAPAR over the US-Me5 site [44,437°N;

-121,56°E], associated with regime 3 are shown in the top left hand side panel on Figure 17. The two main interesting findings are that 1) both sources of information indicate no strong seasonal cycle, as could be expected over this ponderosa pine conifer forest, and 2) the discrepancy in the FAPAR amplitudes between space and ground-based datasets is extremely high (about a factor of 2). Both TIP and QA4ECV products show same amplitude of values whereas AVH15 do not provide values, maybe because of no expected values are retrieved. Interestingly this is a typical class of vegetated canopies deviating significantly from the 1-D statistically homogeneous situation. In that instance, the classical Beer-Bouguer-Lambert law of exponential attenuation applies only if the 3-D radiative effects are adequately parameterised which is not the case in the ground-based measurements.

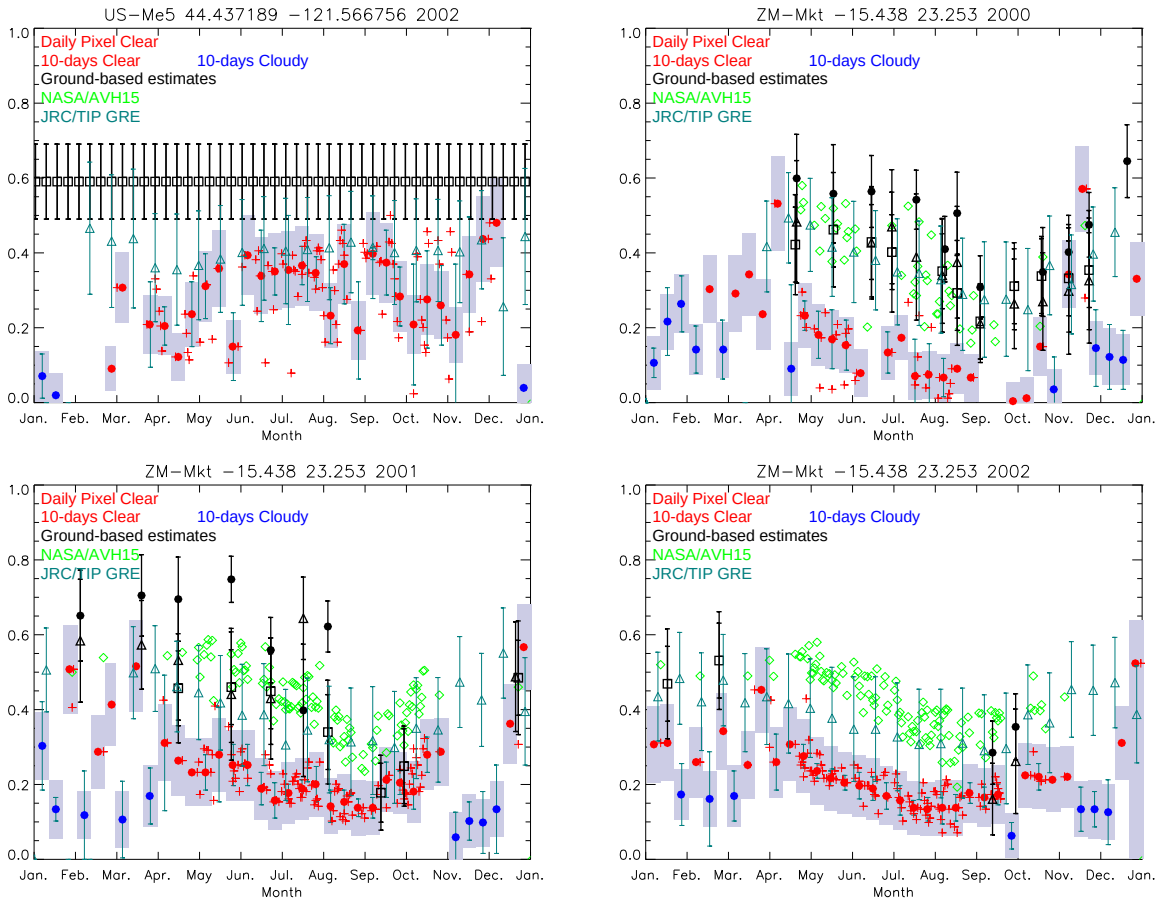

Figure 17: Time series associated with radiation transfer regime 3.

The additional ground-based dataset associated with regime 3, identified in Table 2 is over ZM-Mkt [-15,438°N; 23.253°E], derives from a collection and analysis of the canopy gap fraction using the TRAC instrument over two consecutive years in a mixed shrub-land/woodland environment. Figure 17 (top right hand side and bottom panels) shows the time series of the space FAPAR products for year 2000, 2001 and 2002 together with the measurements (in terms of FAPAR spatial averages and associated standard deviations) collected by the TRAC instrument over three transects of 750 m at a spatial resolution of about 1.7 cm. These data include a numerically small correction to account for the 3D contributions. During both wet seasons, that is, approximately from September to January, the agreement between space data and ground-based estimations is good. By contrast, AVHRR QA4ECV FAPAR products are systematically biased low, by about 0.2 on average, during the two dry seasons, although the uncertainty ranges of both estimations do overlap and the correlation between the two estimations always remains quite high. This is not the case with the JRC TIP and AVH15 products as their values agree well with ground-based measurements. One may keep in mind that the remaining contamination of the FIPAR measurements by the woody (non-green) elements of the canopy favours the occurrence of a bias gretear than 0.1 with respect to the QA4ECV FAPAR values as shown in Figure 4. This feature is expected to be higher during dry seasons when the relative contribution to the extinction process by the leaves only is decreasing, especially with such a low density canopy (the $\langle LAI \rangle$ varies approximately in the range [1-1.5] during the dry seasons (Privette et al., 2004)).

5 Global product comparisons against SeaWiFS data

This section presents the comparison between QA4ECV and JRC SeaWiFS products at two temporal and spatial scales. The first exercise focuses on the daily products ar $0.05^\circ \times 0.05^\circ$ whereas the second analysis presents the comparisons of monthly products at $0.5^\circ \times 0.5^\circ$. This latter analysis shows that, despite a bias, both long time series can be used together by applying a bias correction as done in (Gobron and Robustelli, 2013) for global change studies.

5.1 Daily products at $0.05^\circ \times 0.05^\circ$

Daily QA4ECV AVHRR FAPAR products are benchmarked against SeaWiFS over two years, *i.e.* 1999 and 2003. SeaWiFS products are derived using the same type of land retrieval method (Gobron et al., 2002a, Gobron et al., 2006c) except that the inputs are from the top of atmosphere measurements.

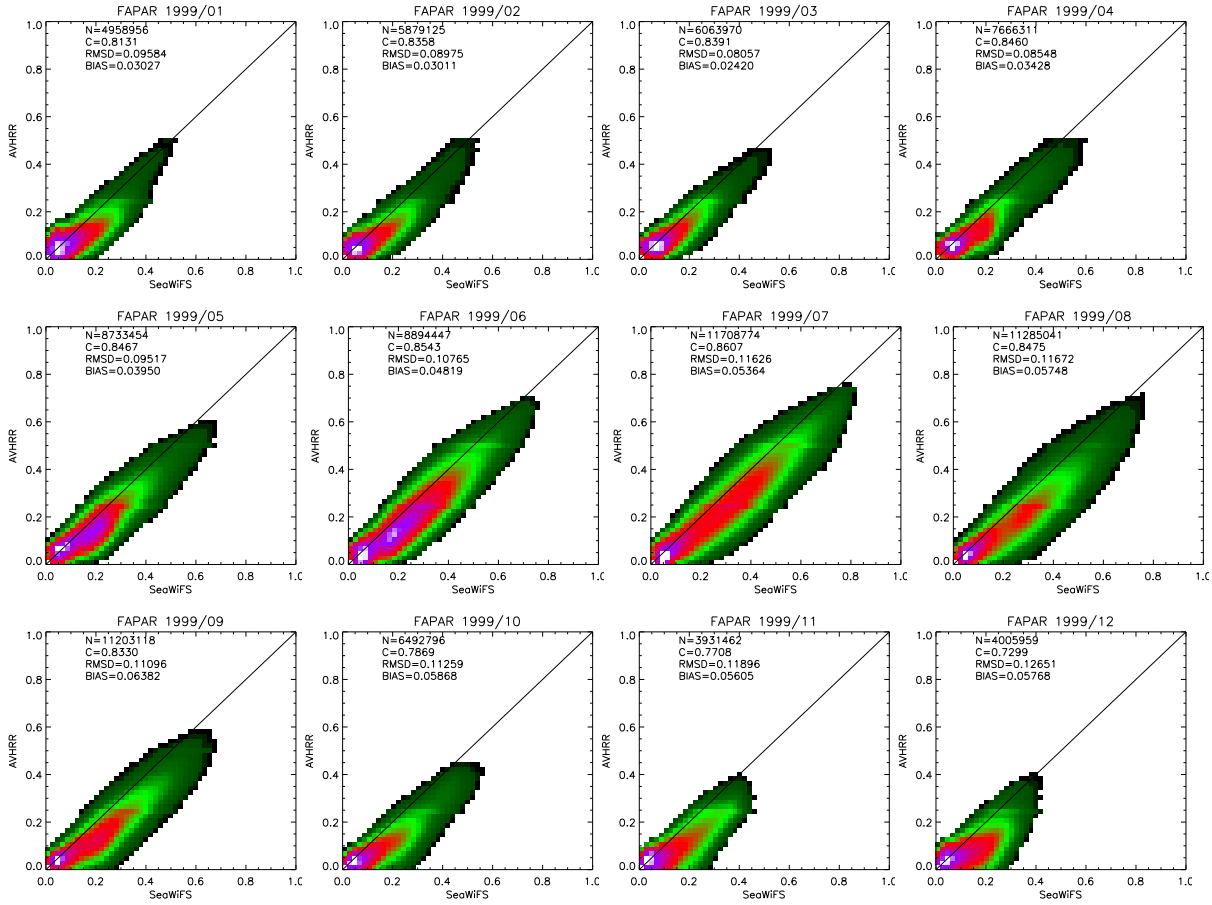

Figure 18: Direct comparisons between daily AVHRR and SeaWiFS FAPAR products in 1999. Only valid grid-cells for which JRC flag in AVHRR products is set to vegetated area and where there is less than 50% of clouds in SeaWiFS ones are plotted.

In order to minimise the impact of remaining cloud effects in AVHRR dataset (such as the red dotted points in previous section) and in SeaWiFS aggregated products, data are filtered by keeping only the grid cells that contain less than 50% of cloudy pixels at 1km. Figures 18 and 19 show the scatter-plots for individual month in 1999 and 2003, respectively.

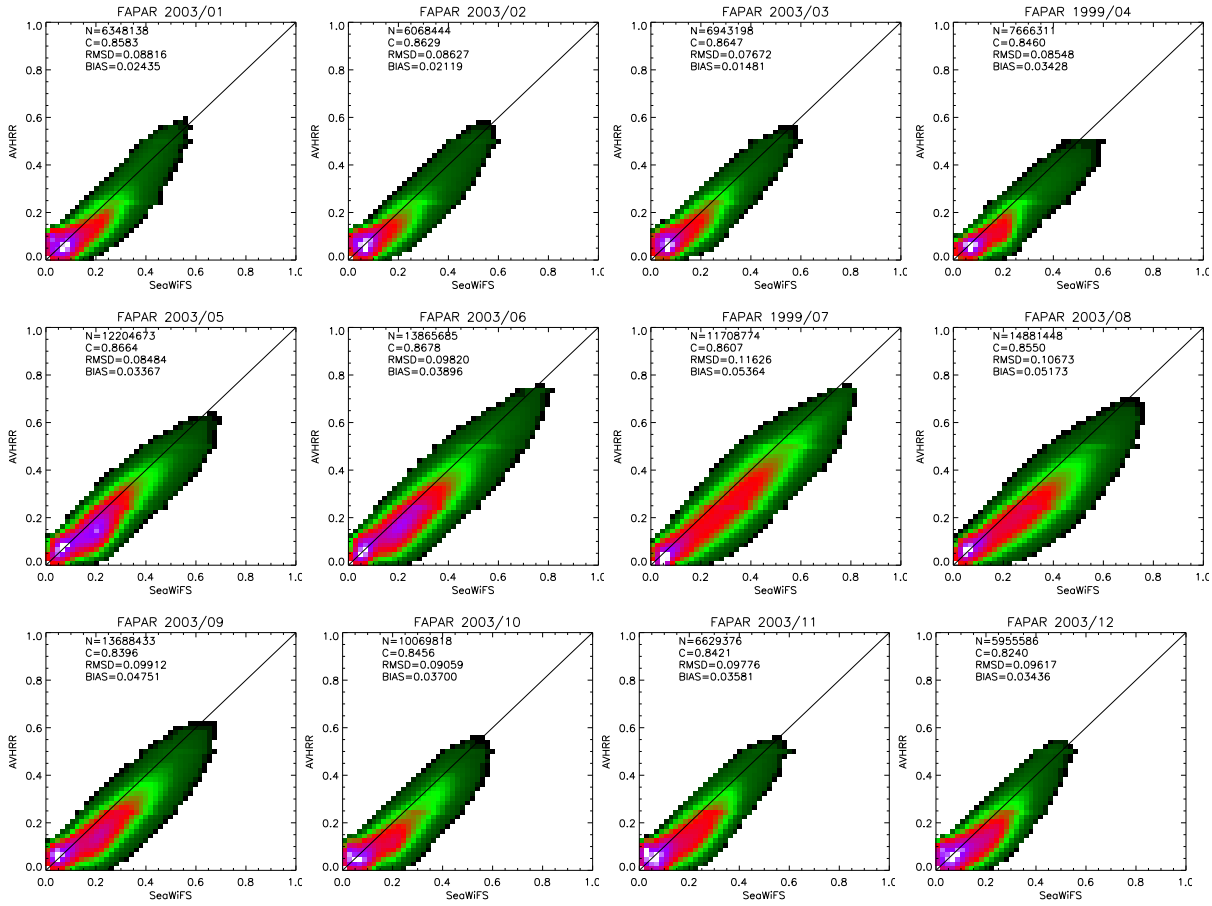

Figure 19: Direct comparisons between daily AVHRR and SeaWiFS FAPAR products in 2003. Only valid grid-cells for which JRC flag in AVHRR products is set to vegetated area and where there is less than 50% of clouds in SeaWiGS ones are plotted.

Daily statistics are reported in Figures 20 and 21. Bias and RMSD are plotted in red and pink colour, respectively. In addition the spatial standard deviation within SeaWiFS is displayed in green whereas the uncertainties of AVHRR FAPAR in blue. We can see that for 1999 and 2003, bias (RMSD) values are lower than 0.05 (0.10) during winter days but increase during summer days. These values are always smaller when comparing against the actual uncertainties of FAPAR, *i.e.* σ, except over various month for the RMSD. The spatial deviation within SeaWiFS values at the same order of the uncertainties of daily AVHRR FAPAR. In 1999, both values of bias and RMSD are higher comparing to 2003, this may be due to inter-calibration bias between platform NOAA14 and NOAA16.

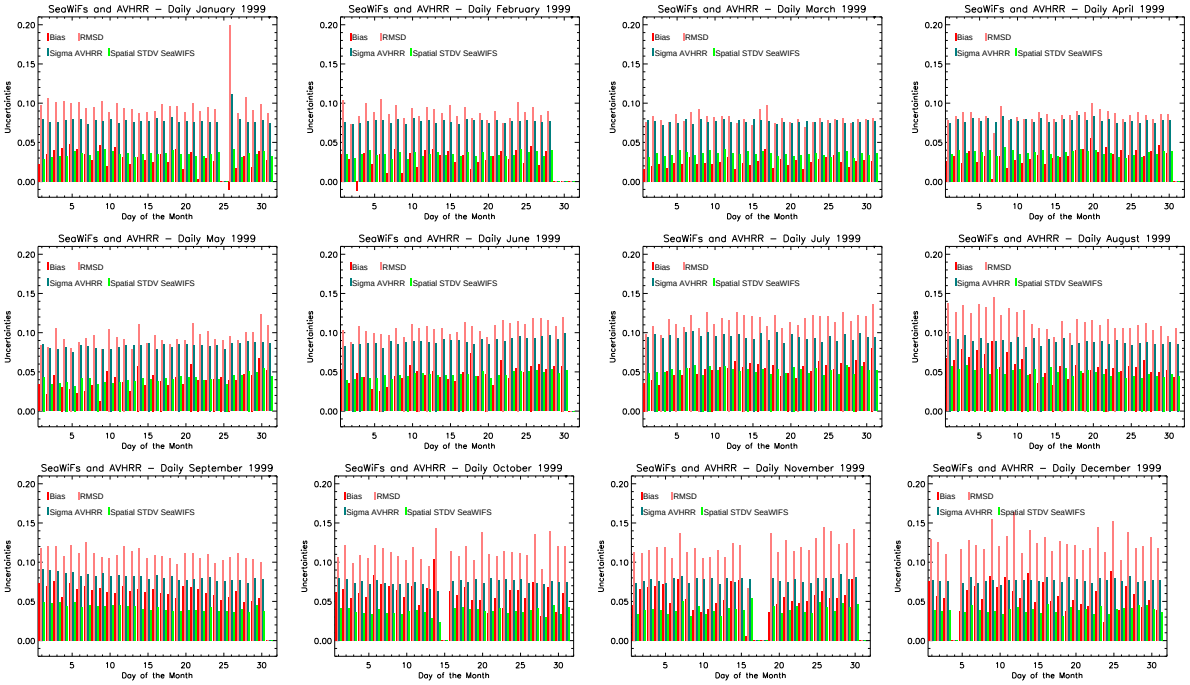

Figure 20: Daily bias and RMSE in 1999

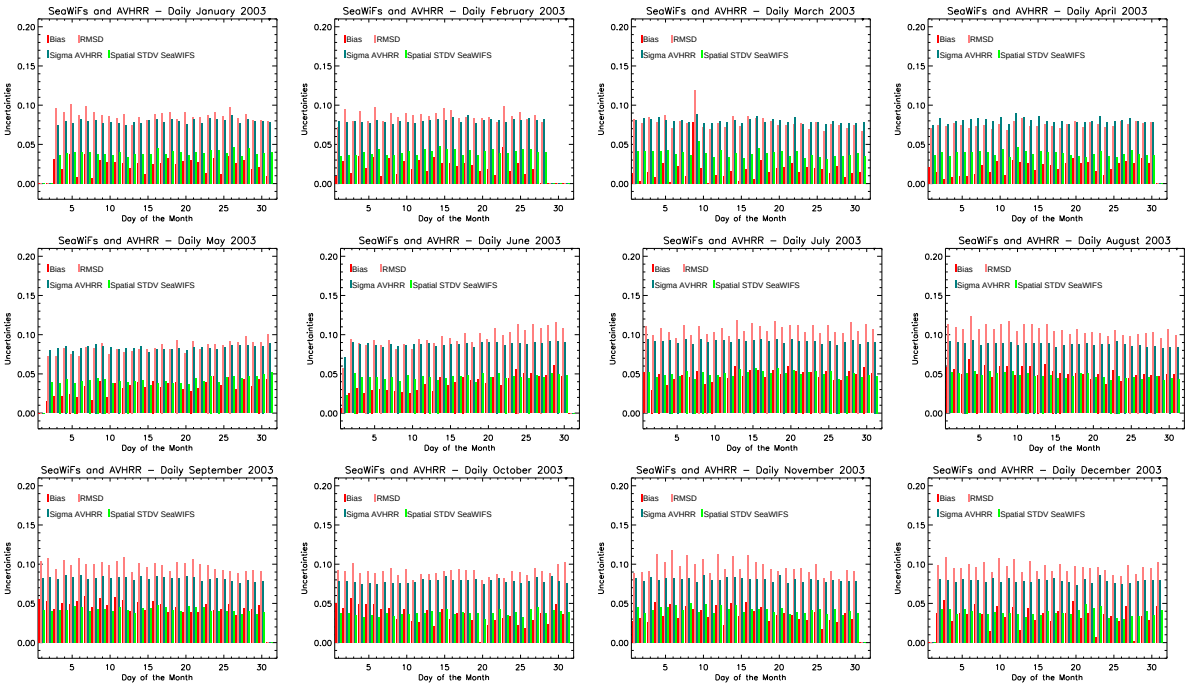

Figure 21: Daily bias and RMSE in 2003

5.2 Monthly products at $0.5^\circ \times 0.5^\circ$

This subsection displays the mean average bias between SeaWiFS and AVHRR monthly products at $0.5^\circ \times 0.5^\circ$over 1998-2003 period. Figure 22 illustrates the monthly mean bias over the globe for individual month. Reddish (blueish) colour shows negative (positive) values. In general SeaWiFS FAPAR values are lower over lower vegetated canopies, such as over Australia and south of Africa, mainly during north hemisphere winter season and higher over other land cover types.

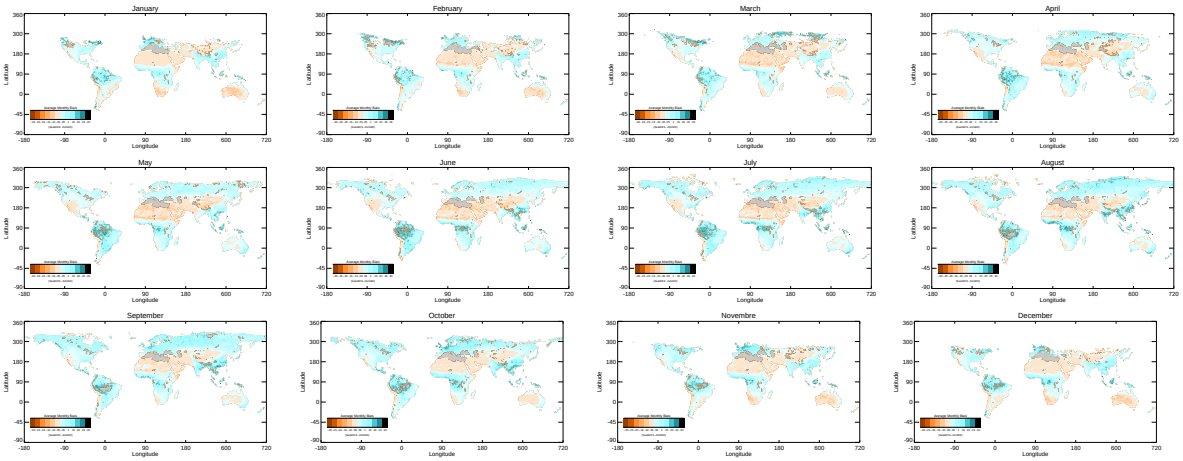

Figure 22: Average monthly bias between SeaWiFS and AVHRR FAPAR over 1998-2003

A monthly pixel by pixel bias correction is applied for rectifying the AVHRR monthly products to further use them together. Figure 23 shows the scatterplot of 12 months by 6 years with histogram of differences. We can see that the mean difference $< \delta >$ is at -0.09 with $\sigma = 0.0974$. When we apply the correction using values of maps displayed in Figure 22, the comparison show the reduced scatters in Figure 24 where $< \delta >$ drops to 0.0002 and $\sigma = 0.0449$.

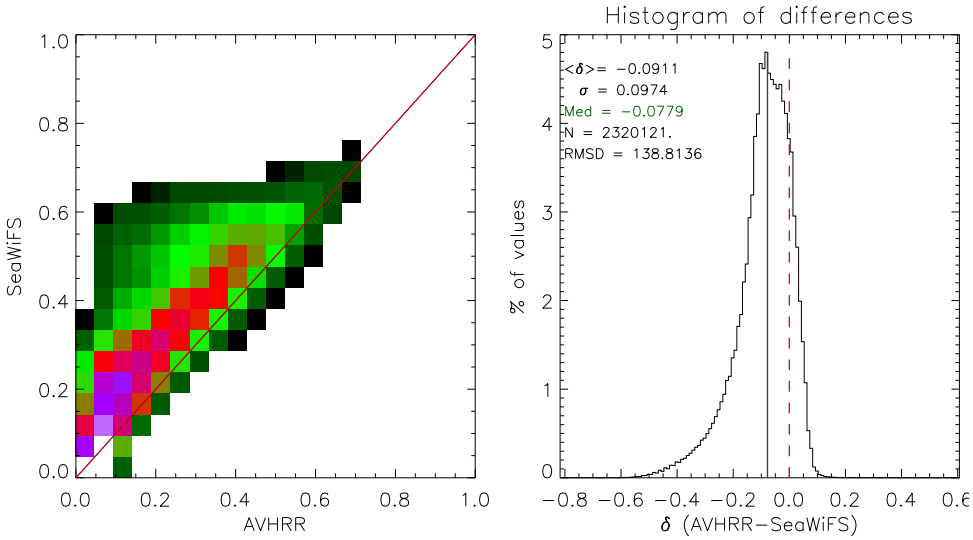

Figure 23: Scatterplots between monthly SeaWiFS and AVHRR FAPAR over 1998-2003.

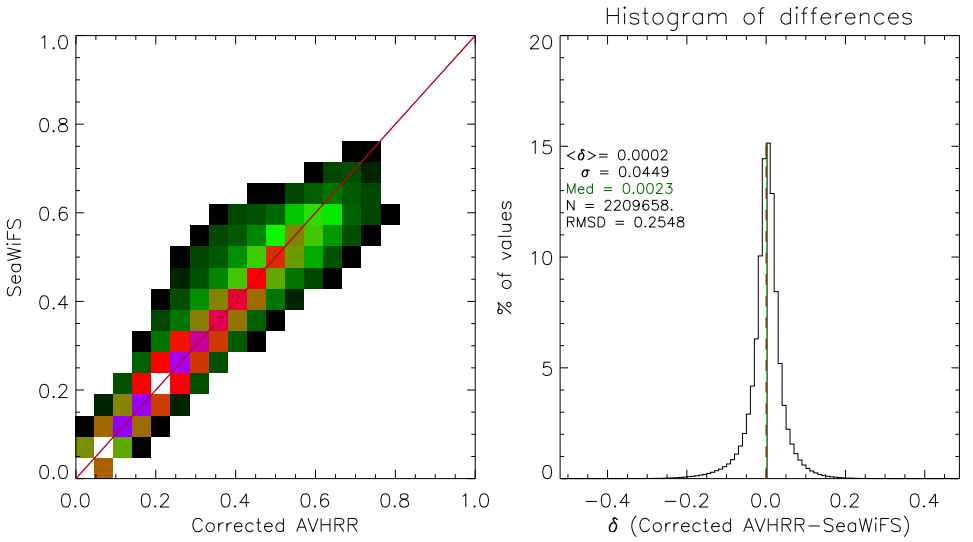

Figure 24: Scatterplots between monthly SeaWiFS and Corrected AVHRR FAPAR over 1998-2003.

6 Conclusion

In this report, we validate and check the quality of the QA4ECV black-sky FAPAR long time series products at $0.05^\circ \times 0.05^\circ$ and $0.5^\circ \times 0.5^\circ$ at either daily, 10-days and monthly period.

Over the QA4ECV validation sites, defined in (Gobron et al., 2015), monthly products at $0.05^\circ \times 0.05^\circ$ from 1982 to 2006 are used to check inter-annual variations and to identify outliers. Moreover the 10-days products are compared over 2003-2004 against the 16-days JRC TIP (using MODIS surface albedo Collection 6 as inputs and under 'green' foliage assumption) and their comparison shows that both products seasonality is well retrieved except when snow and cloud contamination exists. Their level of divergence is within the expected one due to various assumptions in their retrieval algorithm, mainly from diffuse and direct definitions.

Validation, through comparison against time-series of past in-situ data together with LTDR AVHRR FAPAR products and TIP, is presented using the categorisation of the ground-based FAPAR datasets according to their most probable radiative transfer regimes. Due to the spatial scale change between these ground-based measurements and QA4ECV products, we find a relatively good agreement. Further additional analysis are however needed to take into account of the spatial scale deviation.

We compare the global 10-days products against SeaWiFS ones for two years, *i.e.* 1999 and 2003 at $0.05^\circ \times 0.05^\circ$. Both bias and Root Mean Square Deviation (RMSD) are reported together with AVHRR FAPAR uncertainties and the spatial standard deviation of SeaWiFS and we find larger differences in 1999 than in 2003. However both bias and RMSD values are at the same order that the QA4ECV uncertainties.

The last section shows that monthly bias at $0.5^\circ \times 0.5^\circ$ can be used to correct the QA4ECV AVHRR black-sky FAPAR products for future analysis of global change over terrestrial surfaces.

References

Claverie, M., Matthews, J. L., Vermote, E. F. and Justice, C. O., 'A 30+ year avhrr lai and fapar climate data record: Algorithm description and validation', *Remote Sensing*, Vol. 8, No 3, 2016. ISSN 2072-4292. . URL http://www.mdpi.com/2072-4292/8/3/263.

Davis, A. B. and Marshak, A., 'Photon propagation in heterogeneous optical media with spatial correlations: Enhanced mean free-paths and wider-than-exponential free-path distributions', *Journal of Quantitative Spectroscopy and Radiative Transfer*, Vol. 84, 2004, pp. 3–34.

Fensholt, R., Sandholt, I. and Rasmussen, M. S., 'Evaluation of MODIS LAI, fAPAR and the relation between fAPAR and NDVI in a semi-arid environment using in situ measurements', *Remote Sensing of Environment*, Vol. 91, 2004, pp. 490–507.

Franch, B., Vermote, E. F., Roger, J.-C., Murphy, E., Becker-Reshef, I., Justice, C., Claverie, M., Nagol, J., Csiszar, I., Meyer, D., Baret, F., Masuoka, E., Wolfe, R. and Devadiga, S., 'A 30+ year avhrr land surface reflectance climate data record and its application to wheat yield monitoring', *Remote Sensing*, Vol. 9, No 3, 2017. ISSN 2072-4292. . URL http://www.mdpi.com/2072-4292/9/3/296.

GCOS, 'he Global Observing System for Climate: Implementation Needs', Tech. Rep. GCOS-200, World Meteorological Organization, 2003.

GCOS, 'Summary Report of the eleventh session of the WMO-IOC-UNEP-ICSU (WMO/TD-No.1189)', Report Melbourne, Australia, April 7-10 GCOS-87, World Meteorological Organization, 2016.

Gobron, N., 'Envisat's medium resolution imaging spectrometer (meris) algorithm theoretical basis document: Fapar and rectified channels over terrestrial surfaces', Scientific and Technical Report EUR Report 24844 EN, 2011a.

Gobron, N., 'Ocean and Land Colour Instrument (OLCI) FAPAR and Rectified Channels over Terrestrial Surfaces Algorithm Theoretical Basis Document ', EUR Report No.xxxxx EN, Institute for Environment and Sustainability, 2011b.

Gobron, N., 'QA4ECV" Algorithm Theoretical Basis Document for JRC AVHRR FAPAR', Eur report, European Commission, 2017.

Gobron, N., Adams, J., Brennan, J., Disney, M., Govaerts, Y. and Mio, C., 'QA4ECV: Descriptions of virtual validation sites', Report JRC97694, European Commission, 2015.

Gobron, N., Aussédat, O. and Pinty, B., 'MODerate resolution Imaging Spectroradiometer (MODIS) - JRC-FAPAR at 250m Algorithm Theoretical Basis Document', EUR Report 22279 EN, European Commission - DG Joint Research Centre, Institute for Environment and Sustainability, 2006a.

Gobron, N., Aussédat, O. and Pinty, B., 'MODerate Resolution Imaging Spectroradiometer (MODIS), JRC-FAPAR Algorithm Theoretical Basis Document', EUR Report No. 22164 EN, Institute for Environment and Sustainability, 2006b.

Gobron, N., Aussédat, O., Pinty, B., Taberner, M. and Verstraete, M. M., 'Medium Resolution Imaging Spectrometer (MERIS) - Level 2 Land Surface Products - Algorithm Theoretical Basis Document-Revision 3.0', EUR Report No.21387 EN, Institute for Environment and Sustainability, 2004.

Gobron, N., Pinty, B., Aussedat, O., Chen, J. M., Cohen, W. B., Fensholt, R., Gond, V., Huemmrich, K. F., Lavergne, T., Mélin, F., Privette, J. L., Sandholt, I., Taberner, M., Turner, D. P., Verstraete, M. and Widlowski, J.-l., 'Evaluation of FAPAR Products for Different Canopy Radiation Transfer Regimes: Methodology and Results using JRC Products Derived from SeaWiFS against ground-based estimations.', *Journal of Geophysical Research Atmospheres*, Vol. 111, 2006c, D131110. .

Gobron, N., Pinty, B., Aussédat, O., Taberner, M., Faber, O., Mélin, F., Lavergne, T., Robustelli, M. and Snoeij, P., 'Uncertainty estimates for the FAPAR operational products derived from MERIS - Impact of top-of-atmosphere radiance uncertainties and validation with field data', *Remote Sensing of Environment*, Vol. 112, 2008, pp. 1871–1883. .

Gobron, N., Pinty, B., Mélin, F., Taberner, M. and Verstraete, M. M., 'Sea Wide Field-of-View Sensor (SeaWiFS) - An optimized FAPAR algorithm - Theoretical Basis Document', EUR Report No.20148 EN, Institute for Environment and Sustainability, 2002a.

Gobron, N., Pinty, B., Verstraete, M. M. and Taberner, M., 'Global Land Imager (GLI) - An optimized FAPAR algorithm - Theoretical Basis Document', EUR Report No.20147 EN, Institute for Environment and Sustainability, 2002b.

Gobron, N., Pinty, B., Verstraete, M. M. and Taberner, M., 'VEGETATION - An optimized FAPAR algorithm - Theoretical Basis Document', EUR Report No.20146 EN, Institute for Environment and Sustainability, 2002c.

Gobron, N. and Robustelli, M., 'Monitoring the state of the global terrestrial surfaces', In 'Ouwehand L.(ed.) Proceeding of the 2013 ESA Living Planet Symposium, 9-13 September 2013, Edinburgh, UK, Issue SP-722, ISBN 978-92-9221-286-5', .

Gobron, N. and Verstraete, M., 'FAPAR, ECV-T11: GTOS Assessment of the status of the development of standards for the Terrestrial Essential Climate Variables', ECV-T11, FAO, Rome, 2009.

Gond, V., de Pury, D. D. D., Veroustraete, F. and Ceulemans, R., 'Seasonal variations in leaf area index, leaf chlorophyll, and water content; scaling-up to estimate fAPAR and carbon balance in a multilayer, multispecies temperate forest', *Tree Physiology*, Vol. 19, 1999, pp. 673–679.

Huemmrich, K. F., Privette, J. L., Mukelabai, M., Myneni, R. B. and Knyazikhin, Y., 'Time-series validation of MODIS land biophysical products in a Kalahari woodland, Africa', *International Journal of Remote Sensing*, Vol. 26, 2005, pp. 4381–4398.

Knyazikhin, Y., Martonchik, J., Myneni, D., R.B.and Diner and Running, S., 'Synergistic algorithm for estimating vegetation canopy leaf area index and fraction of absorbed photosynthetically active radiation from modis and misr data.', *Geophys. Res.*, 1998, pp. 32257–32276.

Lanconelli, C., Gobron, N., Adams, J., Danne, O., Blessing, S., Robustelli, M., Kharbouche, S. and Muller, J. P., 'QA4ECV: Report on the Quality Assessment of Land ECV retrieval algorithms', Report JRCXXXX, European Commission, 2017.

Pinty, B., Andredakis, I., Clerici, M., Kaminski, T., Taberner, M., Verstraete, M. M., Gobron, N., Plummer, S. and Widlowski, J.-L., 'Exploiting the MODIS albedos with the Two-stream Inversion Package (JRC-TIP): 1. Effective leaf area index, vegetation, and soil properties', *Journal of Geophysical Research Atmospheres*, Vol. 116, No D09105, 2011. .

Privette, J., Tian, Y., Roberts, G., Scholes, R., Wang, Y., Caylor, K., Frost, P. and Mukelabai, M., 'Vegetation structure characteristics and relationships of kalahari woodlands and savannas', *Global Change Biology*, Vol. 10, No 3, 2004, pp. 281–291. ISSN 1365-2486. . URL http://dx.doi.org/10.1111/j.1365-2486.2004.00740.x.

QA4EO, 'A guide to establish a Quality Indicator on a satellite sensor derived data product', Document QA4E0-QAEO-GEN-DQK-001, QA4EO-GE0, 2012.

Shabanov, N. V., Wang, Y., Buermann, W., Dong, J., Hoffman, S., Smith, G. R., Tian, Y., Knyazikhin, Y. and Myneni, R. B., 'Effect of foliage spatial heterogeneity in the MODIS LAI and FPAR algorithm over broadleaf forests', *Remote Sensing of Environment*, Vol. 85, 2003, pp. 410–423.

Turner, D. P., Ritts, W. D., Cohen, W. B., Maeirsperger, T., Gower, S. T., Kirschbaum, A., Running, S. W., Zhao, M., Wofsy, S., Dunn, B. L., Campbell, J., Oechel, W., Kwon, c. H., Meyers, T., Small, E., Kurc, S. and Gamon, J., 'Site-level Evaluation of Satellite-based Global Terrestrial GPP and NPP modeling', *Global Change Biology*, Vol. In press, 2004, pp. –.

Wang, Y., Woodcock, C. E., Buermann, W., Stenberg, P., Voipio, P., Smolander, H., Hame, T., Tian, Y., Hu, J., Knyazikhin, Y. and Myneni, R. B., 'Evaluation of the MODIS LAI algorithm at a coniferous forest site in Finland', *Remote Sensing of Environment*, Vol. 91, 2004, pp. 114–127.

List of abbreviations and definitions

AVHRR=Advanced Very High Resolution Radiometer
BRF=Bidirectional Reflectance Factor
BS=Black-Sky
C3S=Copernicus Climate Change Service
CEOS=Committee on Earth Observation Satellites
DHR=Directional-Hemispherical Reflectance
ECV=Essential Climate Variable
EO=Earth Observation
FAPAR=Fraction of Absorbed Photosynthetically Active Radiation
GCOS=Global Climate Observing System
GLI=GLobal Imager
JRC=Joint Research Centre
LAI=Leaf Area Index
LTDR=Land Long Term Data Record
MERIS=Medium Resolution Instrument Sensor
MODIS=Moderate Resolution Imaging Spectroradiometer
NOAA=National Oceanic and Atmospheric Administration
NN=neural networks
OLCI=Ocean Land Colour Instrument
PAR=Photosynthetically Active Radiation
QA=Quality Assurance
QA4EO= Quality Assurance Framework For Earth Observation
QA4ECV=Quality Assurance For Essential Climate Variable
RMSD=Root Mean Square Deviation
RT=Radiative Transfer
SeaWiFS=Sea-viewing Wide Field of View Sensor
TIP=Two-stream Inversion Package
TOA=Top Of Atmosphere

List of figures

List of tables

GETTING IN TOUCH WITH THE EU

In person

All over the European Union there are hundreds of Europe Direct information centres. You can find the address of the centre nearest you at: https://europa.eu/european-union/contact_en

On the phone or by email

Europe Direct is a service that answers your questions about the European Union. You can contact this service:

- by freephone: 00 800 6 7 8 9 10 11 (certain operators may charge for these calls),

- at the following standard number: +32 22999696, or

- by electronic mail via: https://europa.eu/european-union/contact_en

FINDING INFORMATION ABOUT THE EU

Online

Information about the European Union in all the official languages of the EU is available on the Europa website at: https://europa.eu/european-union/index_en

EU publications
You can download or order free and priced EU publications from EU Bookshop at: https://publications.europa.eu/en/publications. Multiple copies of free publications may be obtained by contacting Europe Direct or your local information centre (see https://europa.eu/european-union/contact_en).

KJ-NA-29076-EN-N

The European Commission's science and knowledge service

Joint Research Centre

JRC Mission

As the science and knowledge service of the European Commission, the Joint Research Centre's mission is to support EU policies with independent evidence throughout the whole policy cycle.

EU Science Hub

ec.europa.eu/jrc

@EU_ScienceHub

EU Science Hub - Joint Research Centre

Joint Research Centre

EU Science Hub

Publications Office

doi:10.2760/28321

ISBN 978-92-79-77731-8